Sensing Systems for Glass Ceramic Cooktops

A Summary of Results from Several Collaborative Projects with Schott Glass

Joseph Paradiso, Lance Borque, Philip Bramson, Mat Laibowitz, Hong Ma, Mat Malinowski
Responsive Environments Group
MIT Media Lab

July 18, 2003

Introduction to Sensing Systems for Cooktops

Prof. Joseph A. Paradiso

On August 23 of 2002, I spent the day in meetings with TTT colleagues at Schott Glass in Mainz, Germany. The meetings were organized in a workshop format, with the purpose of generating ideas for collaborative projects between the Media Lab and Schott. The day was quite productive, and resulted in 9 possible projects.

The more desirable and easier projects were targeted, and upon returning to MIT, I assigned students to them. Most of these projects were done by UROPs (paid undergraduate researchers), with contributions from RA's where appropriate. Although they provided the undergraduates with good experience, gave them a creative outlet, and were somewhat fun, I couldn't see any evolving into theses yet, hence were perfect for the UROPs. The primary student responsible for each project produced a report summarizing their results. A quick executive summary is given below with the contributing students listed, and their detailed reports are appended.

1) Wake up electronics without stand-by power - Hong Ma

As Schott's capacitive button electronics consume too much power for standby limits under new EU regulations, we adapted our ultra low power wakeup electronics from the FindIT Flashlight project (see: http://www.media.mit.edu/resenv/pubs/papers/2002-10-UbiComp-FindIT.pdf), using a microphone (which replaced the photosensor on the Flashlight's tags), mounted under a piece of glass ceramic to

detect vibrations when the glass was touched, activating a processor that then could wake up the capacitive sensing electronics. This was quite successful - the system ran in standby using under 500 nA and was able to wake up reliably when the glass was lightly tapped. This demo was given to Schott in October of 2002.

2) Haptic feedback on touchsensors - Mat Laibowitz

Schott expressed an interest in exploring some kind of vibratory response when the glass ceramic buttons were touched - a problem with the capacitive buttons is that they work by pure touch, and exhibit no kind of haptic signature when pushed, as mechanical buttons do. Mat Laibowitz modified a Schott touch button array with a pager motor epoxied to the underside of the glass ceramic, and programmed a PIC microcontroller to drive it with a variety of different pulse effects when the buttons were contacted. This worked nicely, and was demoed to Schott in October of 2002. The demo hardware was subsequently given to Sile O'Moudrain at MLE, who engaged her students in refining it further, using different haptic actuators and varuous kinds of stimuli. This demo was given to Schott in the winter of 2003.

3) Linear Slider Control - Lance Borque

As the capacitive controls currently used on glass ceramic cooktops employ only discrete buttons, we decided to explore the development of a continuous capacitive slider. Rather, for example, than setting heat of a burner using increment-decrement hits on one button, one can now just slide one's finger along a line, adjusting the heat continuously as one does on a conventional analog stove control. Lance Borque exploited an interdigitated dual electrode structure to do this. The system has been demoed to Schott on several occasions as it evolved during the spring of 2003 - the background effect from rolling the finger that Thomas Zenker noted during his visit a few weeks ago has now been removed by shielding the common electrodes on either side of the interdigitated structure, and it works quite nicely. A demo video can be seen at http://www.media.mit.edu/~joep/MPEGs/CeranSlider.mov , and the demo will be given to Schott later this summer.

4) Capacitive Pot Detection - Philip Bramsen, Hong Ma

Schott expressed an interest in detecting the presence, size and position of pots on the cooktop. Philip Bramsen developed two techniques to do this - one using capacitive loading of the pot and employing the shield on the burner as an electrode, and the other employing an array of electrodes under the glass ceramic to exploit transmit-receive capacitive coupling. Although both techniques functioned, the transmit-receive configuration was superior (and as the electrodes are high-impedance, they can be routed off the cooktop with a simple connection mechanism - much simpler than a plated burner, for example). There is an effect, however, when the pot is contacted. Although this inhibits the system

from working properly when the pot is touched, the signal is quite dramatic, however and seems able to be distinguished from other situations easily, potentially giving additional information (e.,g., the user is touching the pot or stirring the pot with a conductive stirrer). This system was demoed to Schott in July of 2003.

5) Temperature sensing through the glass ceramic via PIR - Hong Ma, Philip Bramsen

Schott expressed an interest in remotely measuring the temperature of the glass ceramic surface above a burner. As optical lines of sight, etc. can be difficult for standard PIR thermometers, Schott was interested in sensing temperature through the glass ceramic. As the glass ceramic is 80% transparent for light between 1.3 and 2.7 microns in wavelength (well into IR), a photodiode sensitive in that region can be mounted on the edge of the glass ceramic, looking through the cooktop at the burner to ascertain its temperature though black body radiation. Hong Ma and Philip Bramsen developed a system to do this, and it seems to work. In practical implementation, one would need to appropriately shield and/or temperature compensate the photodiodes (we do that now with dual detectors, but there's probably a simpler way), and issues of attenuation in the glass causing a perceived temperature drop as the burner is moved away from the detector would need to be calibrated out.

6) Remote temperature, liquid, and pot sensing using ultrasound in the glass - Mat Malinowski

In discussions with Schott, there was considerable excitement at the idea of remotely sensing temperature and possibly other parameters through the glass using ultrasound. Accordingly, Mat Malinowski epoxied a pair of PZT ultrasound transducers onto opposite ends of a piece of glass ceramic, driving one with brief pulses of sinusoidal excitation at various frequencies while receiving at the other. Although predictions from variation of the coefficients of elasticity and expansion in glass ceramic with temperature indicate little or no effect, Mat detected a phase shift that increased uniformly with temperature in his received signal. The main effect, however, seemed to be seen in the multipath signal that arrived after the prompt transmission. Accordingly, this technique could be sensitive to the cooktop geometry, or even worse, due to some kind of background. Although this prevents us from making any claims here (especially since we don't yet understand the mechanism underlying these phenomena), Mat's results are tantalizing, and will be verified with a small electric heater that Thomas will send to us shortly.

UltraLow Power Acoustically Triggered Microprocessor Wakeup

Hong Ma
Responsive Environments Group
MIT Media Lab

We have designed an acoustically triggered sensor mounted on Schott cooktop to wakeup a microprocessor from sleep state. This device is motivated by the desire to minimize ambient power consumption on cooktops in compliance with EU regulations. Our systems is composed an acoustic sensor, a low-power comparator, and a minimalist microprocessor. The acoustic sensor is a contact microphone glued to the surface of an Schott glass cooktop. An acoustic signal from a very light tap or knock on the glass causes a voltage signal to be generated by contact microphone. The voltage signal is put through a high-pass filtered and then discriminated by a, LTC1540, low-power comparator. The output of the comparator goes to wakeup an 8-pin PIC12C509A microprocessor. The overall power consumption is a mere 0.5μa during the ambient state. Figure 1 shows the circuitry – as shown, it's based on a battery-powered supply, but is easily adapted to use a capacitor that is charged when the supply is active.

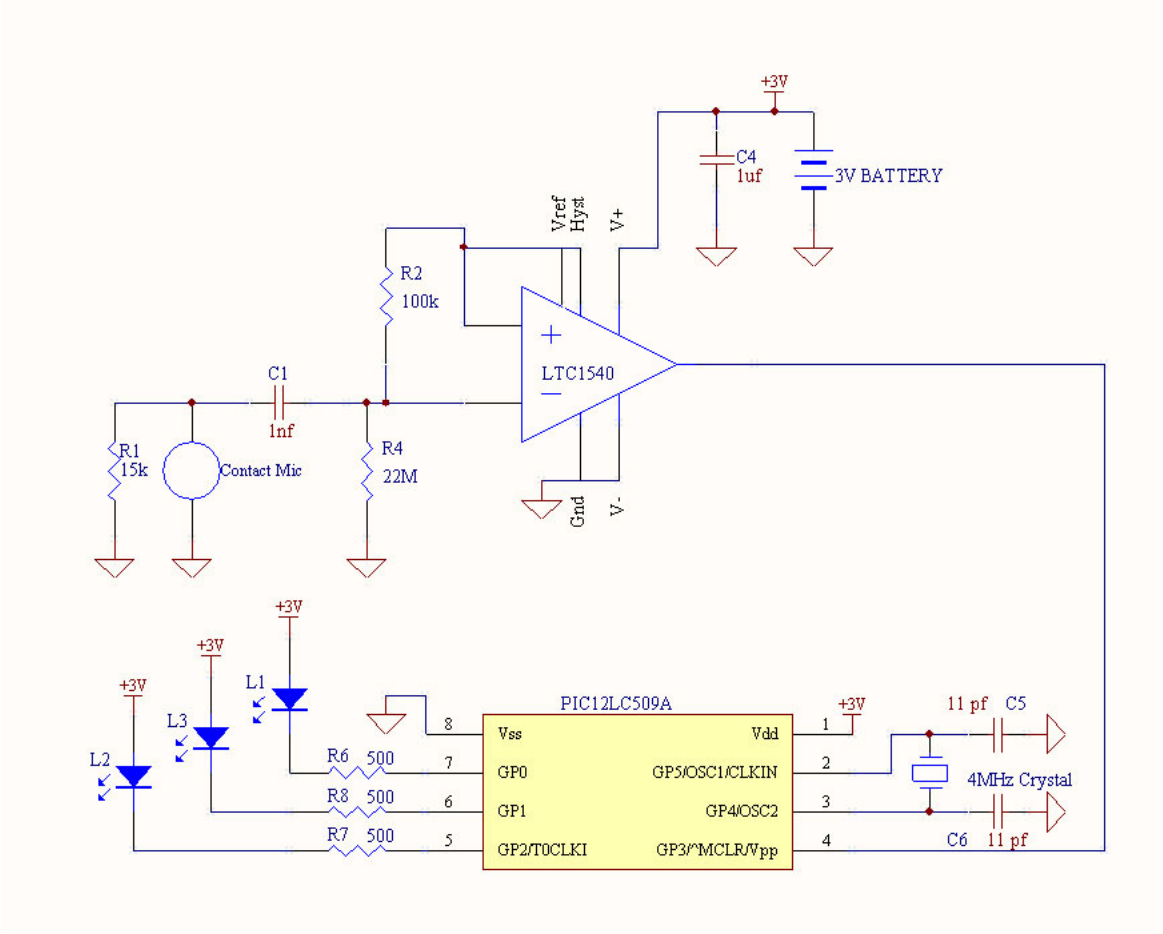

Figure 1: UltraLowPower Acoustic Wakeup Circuit for Cooktop Activation

Haptic Feedback for Touch Sensors

Mat Laibowitz
Responsive Environments Group
MIT Media Lab

The idea of this experiment is to design a method that provides haptic feedback that engages upon the press of a capacitive-based touch sensor switch that otherwise provides no feedback (in contrast to a mechanical switch, which always provides a clear haptic response). This would help to prevent the switch from being triggered unknowingly and make interaction with the switch much more natural. The specific touch switch used here consists of a capacitive sensor positioned under a glass ceramic cooktop labeled with a printed circle denoting the sensor's space. It was a demo that Schott used to demonstrate the cooktop touch switching mechanism.

The glass ceramic proved resistant to propagating vibrations created with an audio-type transducer or with a piezo-based transducer, hence a stronger mechanical actuator was selected. The selected actuator is a sealed vibrating motor in a pancake form factor. This can be easily affixed to the underside of the glass and is resistant of grease and other issue that can arise with a cooktop. It can be run from as low as 3VDC, which allows it to be powered from the same power supply as the sensors. The control circuit, shown in the figure below, consists of a microcontroller, which is interfaced to the sensors, and an N-channel FET to drive the motor. The microcontroller can use PWM to control the amplitude of the vibration of the motor, allowing specific vibration profiles to be designed.

In this demo, two profiles were designed. The first turns the vibration on at a programmable amplitude while the switch is being pressed and turns it off when the switch is released. The second profile is a pulse of vibration when the switch is first pressed, and a second pulse when the switch is released. This is intended to simulate a button press. After demoing this device to Schott in October 2002, it was given to Sile O'Moudrain's Palpable Machines Group at MediaLabEurope, who refined it further, using different actuators and additional pulse sequences, transferring the demo to Schott in March, 2003.

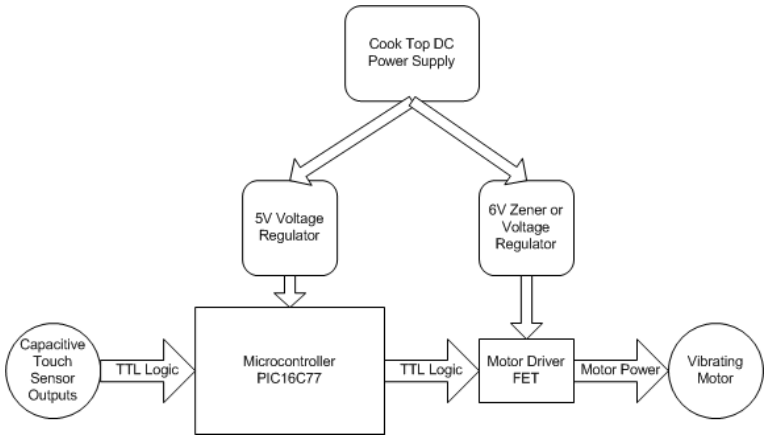

Figure 1: Block Diagram for Haptic Feedback Touch Sensor Demo

A Capacitive Sensor for Tracking Fingertips on Glass Ceramic

Lance Bourque
Responsive Environments Group
MIT Media Lab

July 2003

Abstract

This report details the design of a new capacitive sensor for linearly tracking the movement of a fingertip on the surface of a glass ceramic cooktop. The design exploits the relative stability and predictability of shunt-mode transmit/receive capacitive sensing; loading mode was determined to be erratic in this application. The geometry of the sensor has been optimized to follow the lateral movements of the fingertip over an area of approximately six inches while ignoring other positioning events such as movements of the hand perpendicular to the plane of the sensor or perpendicular to the direction of linear sensing. This is accomplished by using two sensing plates of linearly varying area in close proximity. In conjunction with a differential measurement algorithm, this eliminates the significance of the common-mode variations which would contribute to poor tracking.

1 Capacitive Sensing: Loading-mode and Shunt-mode

In loading-mode capacitive sensing, a transmitting plate is driven with an AC waveform. The plate has a minimal capacitive coupling to ground and only a small amount of current flows into it. The object to be detected must have a strong coupling to ground. When the object is brought near to the transmitter, additional current flows through the transmitter, through the object and on to ground. This increase in current is what is detected.

The first sensor prototype was loading-mode. Although sufficient to show that other modes might work, this method was otherwise inadequate. The sensor had an unacceptable sensitivity to environmental noise and to variations in the loading ability of different people's fingers. Compounding the noise problem was that attempts to shield the sensor with grounded shielding increased the quiescent current to the point where perturbations from fingertips were insignificantly small and impossible to measure.

The present sensor acts in shunt-mode transmit/receive. In this mode there are two plates, a transmitter and a receiver. The transmitter is driven with an AC waveform causing an electric field to form around it. This field couples capacitively to the receiving plate, where the waveform is detected. In shunt mode, the transmitter and the receiver are fixed in space and close to each other, and a large amount of the field is incident on the receiver in the quiescent state. The object to be detected is placed in the field and shunts some field lines away from the receiver. This causes a reduction in the strength of the received signal. This reduction is detected.

This technique has some advantages: firstly, it is very easy to shield the sensor from noise. This is because it is possible to connect the receiving plate to the virtual ground point at the inverting input of an op-amp transimpedance amplifier. With the receiver held at ground, a grounded shield does not adversely affect the response. Secondly, it is possible to tailor the placements of the transmitter, receiver and grounded areas to ensure a significant response localized over the region of interest. Finally, the fact that the transmitter and receiver are in a fixed geometrical relationship causes the operation to be more stable.

2 Sensor Geometry and Principles of Operation

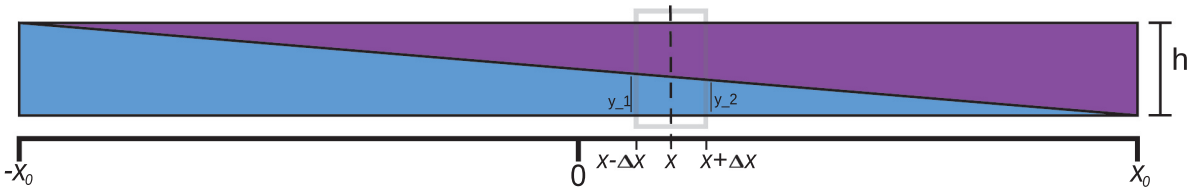

Figure 1: Idealized Geometry

The prototype sensor uses two separate transmitter/receiver pairs in close proximity. Figure 1 shows an idealized illustration of the two receivers. In the diagram, one receiver is in blue, and the other is in purple. They are electrically insulated from each other. Finger tracking is in the x direction. We assume that the electric field from the transmitter is uniformly incident on the receiving plates.

Each sensor is linearly variant in the x direction: the blue occupies the full height of h at point $-x_o$ and tapers linearly to a point at x_o; the purple has its point at $-x_o$ and expands to full height at x_o. In order to understand how position information can be extracted from the sensor, imagine that the fingertip can cover the portion of the receivers under the rectangle centered at point x. This rectangle is of width $2\Delta x$ and covers the entire height h of the two plates. The finger blocks the electric field in proportion to the amount of plate-area covered. For now, remember that since the receivers act independently, the constant of proportionality could be different for each, depending on the gain circuitry in the electronics

which measure current flow in the receivers.

Let the plates be numbered 1 and 2. Then if we take the difference of the field blocked by the two plates and divide it by the sum of the field blocked we have

$$\frac{K_1(Area_1) - K_2(Area_2)}{K_1(Area_1) + K_2(Area_2)}$$

or, due to the geometry,

$$\frac{2\Delta x K_1(\frac{y_1+y_2}{2}) - 2\Delta x K_2(\frac{(h-y_1)+(h-y_2)}{2})}{2\Delta x K_1(\frac{y_1+y_2}{2}) + 2\Delta x K_2(\frac{(h-y_1)+(h-y_2)}{2})}$$

which reduces to

$$\frac{\frac{x}{x_o}(K_1 + K_2) + (K_1 - K_2)}{\frac{x}{x_o}(K_1 - K_2) + (K_1 + k_2)} \ .$$

Finally, in the case where $K_1 = K_2$, this is simply

$$\frac{x}{x_o} \ .$$

And so, using this method, we extract the position of the finger as a number between -1 and 1 and centered at 0. This linear output could be scaled to suit the output indicator. If the gain circuitry is not matched, the linearity suffers, but the effect is slight. Figure 2 shows the response when K_2 is twice K_1.

It is desirable in some applications for the sensor to 'remember' or hold the position where it was last touched after the finger is removed. In order to accomplish this, we notice that for the same Δx, the sum of the signals from the two receivers drops by the same amount regardless of where it is touched. The prototype uses this drop in signal as a triggering event: when the sum drops below a preset threshold, (in the prototype it is 95% of the quiescent sum), tracking begins. When the finger leaves the region of the sensor the sum climbs above threshold, and a microprocessor holds the last calculated position.

Unfortunately, the simplified geometry will not work in the finger-tracking application since it is impossible to guarantee that the full height of the sensor will be covered during tracking: if the finger were moved up, for example, the purple plate would experience a disproportionately large change in incident flux. This would cause a breakdown in the reliability of the position reading. Note however, that changes in the width of the finger, represented in this discussion by $2\Delta x$, are irrelevant since Δx drops out of the formula.

To alleviate the problem of off-axis sensitivity, a modified design of the receivers is used in the prototype. The design appears as figure 3.

In place of side-by-side plates with continuously variable area, we use plates having interdigitated 'fingers' of linearly variable area. If the 'fingers' are small compared with the

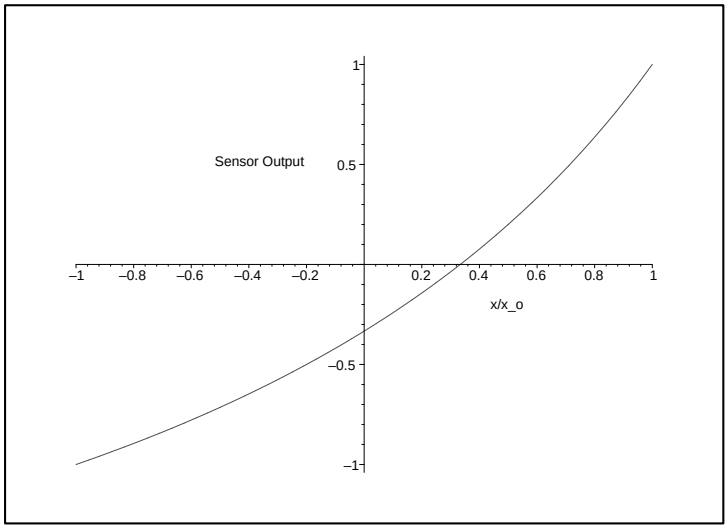

Figure 2: Effect of Gain Mismatch on Linearity

Figure 3: Geometry of the Receivers

width of the flux intercepted during finger tracking, we can make a very good approximation to the ideal linear model. It is easy to so size these plates: in the prototype, the receivers are implemented as printed circuit traces. The smallest 'fingers' are .008 inch wide, and the largest are .15 inch wide. The two plates are separated by a space of .008 inch. The overall length of the sensing area is 6 inches, and the height is 0.5 inch. On each receiver there is a trace of width .008 inch which connects its 'fingers' together. These can be seen extending past the receiving area on the right side of figure 3. These connecting traces are a source of asymmetry in the design and as such must be shielded in a functional sensor.

The complete sensor design must include transmitters, receivers and shielding. The geometry of the prototype appears in figure 4. In the prototype, the receivers are implemented as printed circuit traces, and the transmitters and shielding were applied to the board with copper tape in the same plane as the receivers. The back side of the board is covered with a groundplane. Shielding was also extended over (but insulated from) all connecting traces, leaving only the linearly-varying section of the receivers exposed. The transmitters are 0.25 inch wide and run the length of the sensing region. They are isolated from the receivers by .025 inch of grounded shielding. They are driven by a 50KHz 3Vpp square wave available at a free I/O pin on the microprocessor used to process the position data.

Normal operation of the sensor in the application of finger tracking on glass requires this entire unit to be underneath and pressed firmly against the glass. A stable mechanical mount here improves the stability of the output. The unit also functions without a glass top but the high dielectric constant of the glass reshapes the field lines in such a way as to increase the coupling of the transmitter and receiver and to increase sensitivity to perturbation by a finger.

3 Circuit Details

Though some care must be taken in the circuit layout, complicated electronics are not required for the sensor to function well. Buffering circuitry must be placed as close as possible to the receiving plates in order to maintain good signal strength and noise immunity. The schematic for this front-end is shown in figure 5. The schematic shows the two identical channels necessary to handle both receivers. Each receiver is connected to the inverting input of an op-amp which is held at virtual ground by feedback. Current flowing through the receiver is converted to a voltage at the output of the first op-amp. The feedback resistor is bypassed with a capacitor to prevent runaway gain at high frequencies which would cause instability. After having been converted to a voltage, the signal is AC coupled to a rectifier/low-pass filter where it is converted to DC. The DC voltage is fed to a 12-bit ADC and processed to compute finger position on a microprocessor.

In the prototype the microprocessor also drives a ten-LED bargraph display of the position and sends the digitized voltage readings via serial port to a computer. Here a dedicated display program uses the data to calculate position at a higher resolution. Other relevant

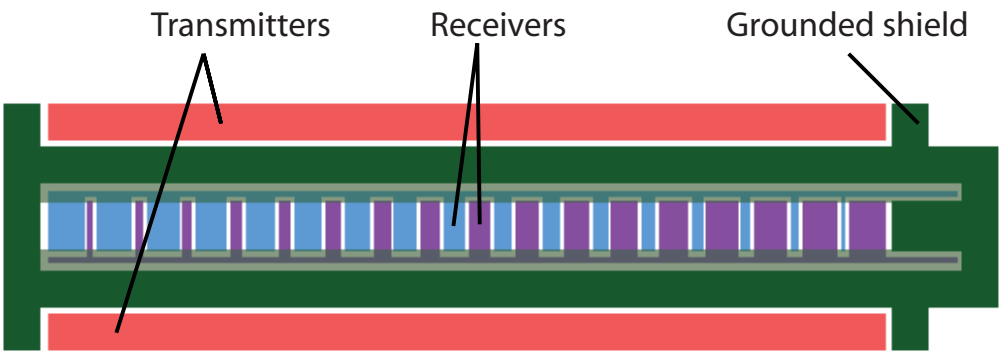

Figure 4: Geometry of Prototype Sensor

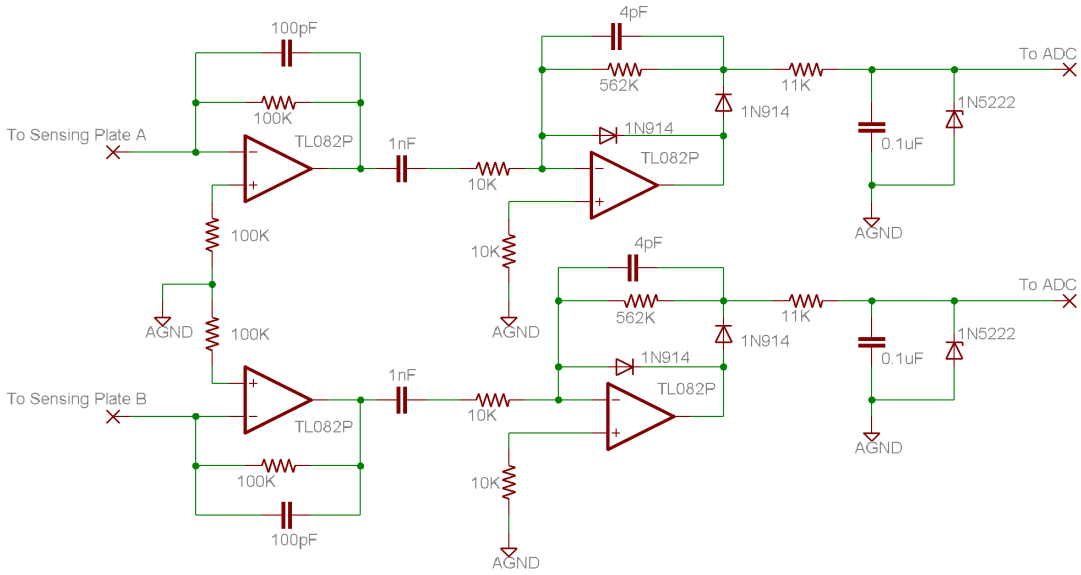

Figure 5: Front-End Schematic

data is also displayed. Screenshots of the display program in operation appear as figure 6.

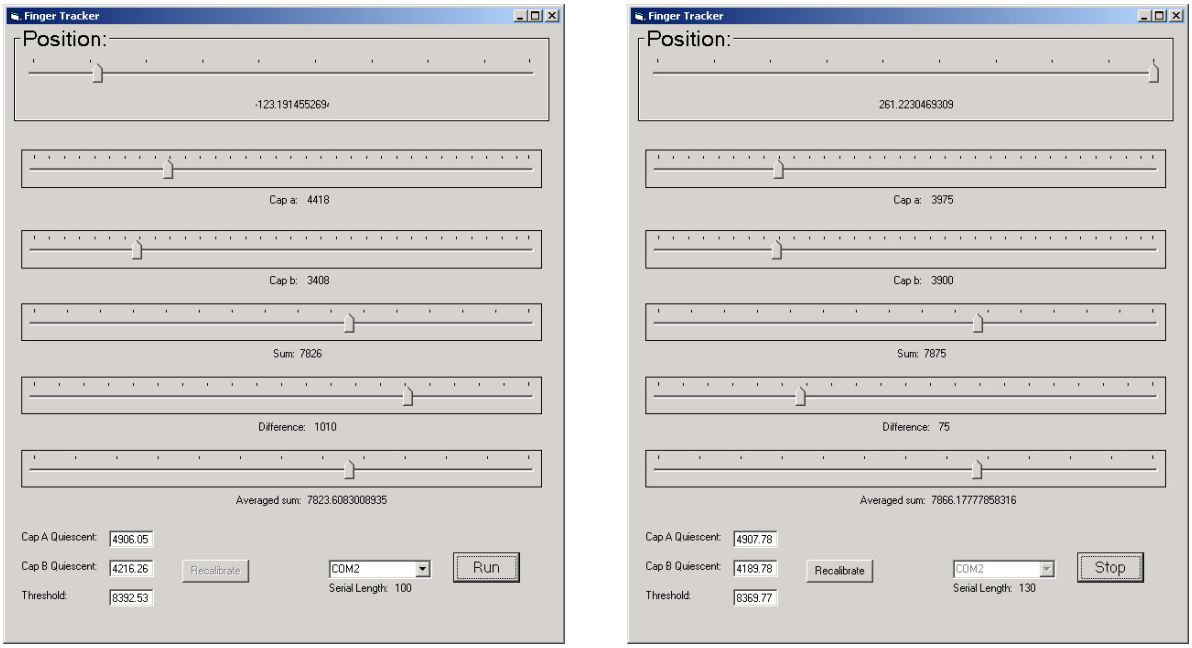

Figure 6: Screenshots of Finger Tracker

4 Conclusion

This design functions well in the application of finger sensing through glass. One slight problem at the current stage is the tendency of the sensor to track the lateral movements of the hand and arm even when the fingertip remains in the same place. This problem arises because a significant amount of flux incident on the receivers has traveled far from the surface of the glass. I believe a good solution to this problem would be to use narrower transmitters located closer to the receivers (but still isolated by a shield). This would cause the field close to the surface of the glass to be dominant.

This slider design was found to be quite insensitive to conductive objects placed atop the glass above the slider electrodes - it wasn't seen to activate until the object was touched. Below are several photographs showing the slider demo.

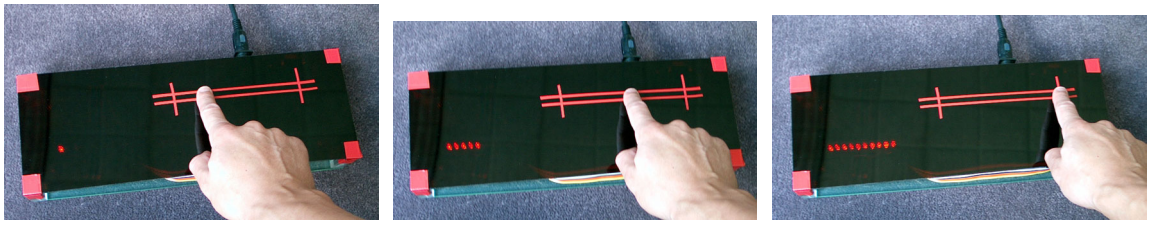

Figure 7: Slider Demo in Action

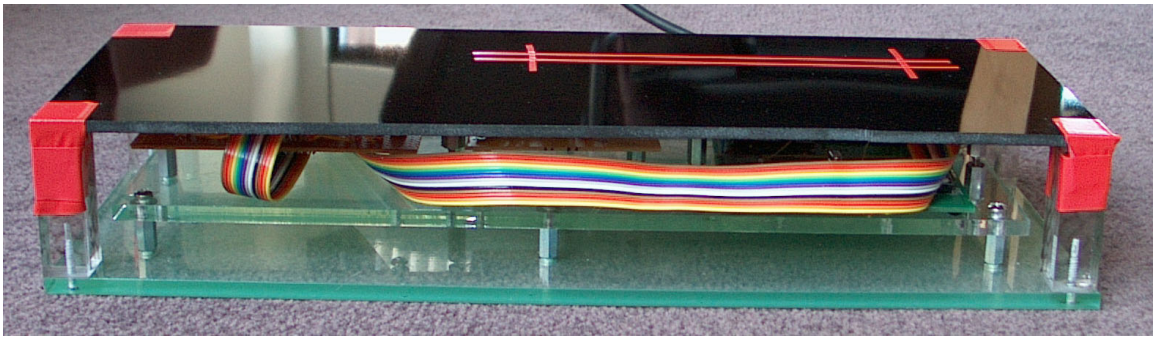

Figure 8: Slider Demo - Edge View

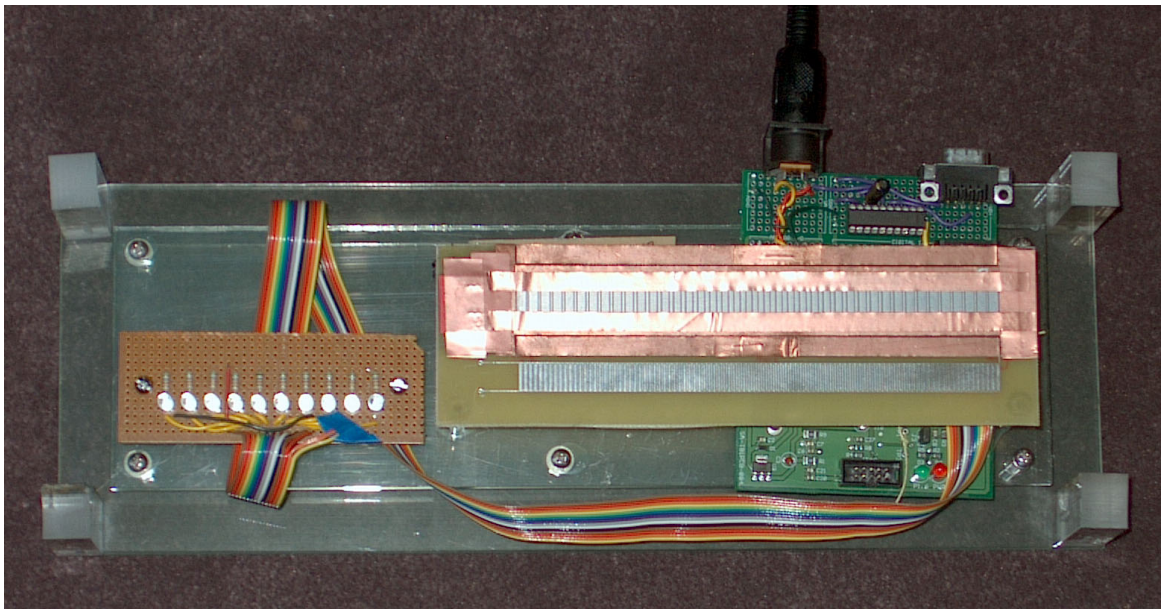

Figure 9: Slider Demo - Glass Cermaic removed to Show Electrodes and Circuitry

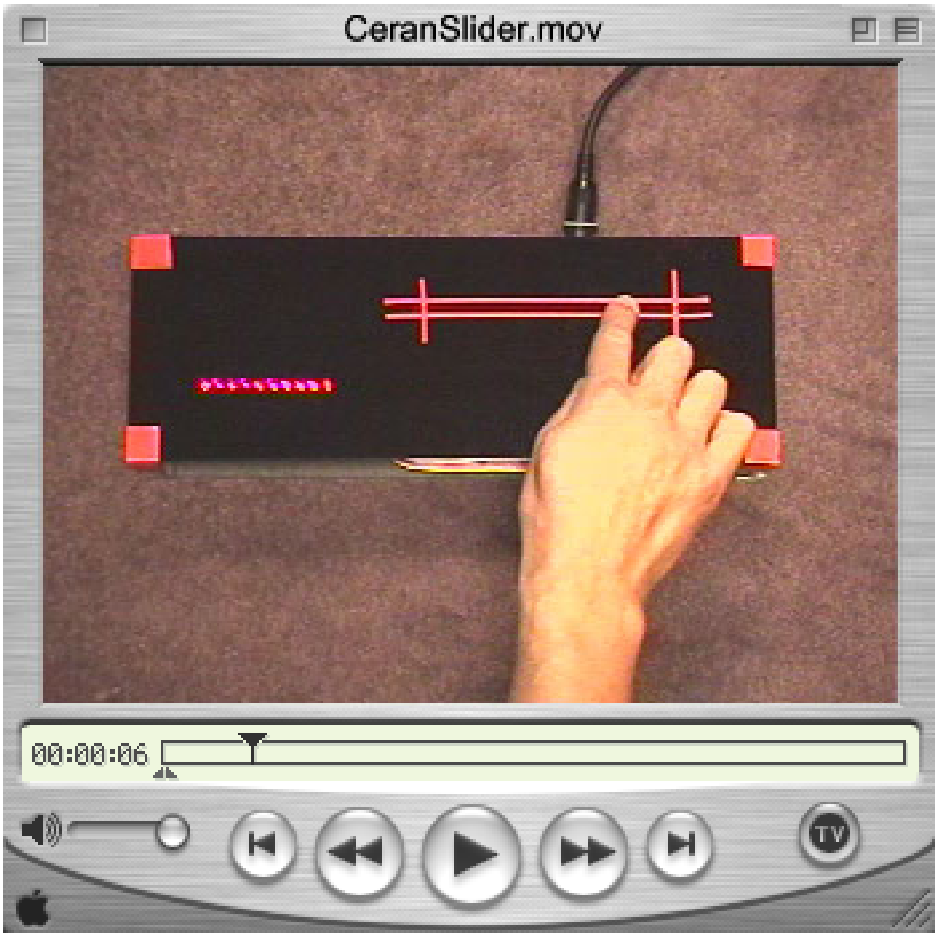

Figure 10: A Video of the Slider Demo can be seen at: http://www.media.mit.edu/~joep/MPEGs/CeranSlider.mov

Capacitive Pot Detection

Philip Bramsen
Responsive Environments Group
MIT Media Lab

Abstract

This report details the design and construction of a pot detector that uses changes in the capacitance of a set of electrodes to infer the size and location of pots on the surface of a cooktop.

Concept

Driving an electrode with a high frequency signal while receiving on second electrode with an opamp circuit dependent on input current yields an output signal dependant on the capacitance of the electrode pair. Placing the plate electrodes against the surface of the glass creates a capacitor strongly dependent upon the presence of a pot above the glass. This is especially effective for a conductive pot, or a pot with conductive contents (e.g., essentially anything used in cooking, so long as it's moist).

Design and Construction

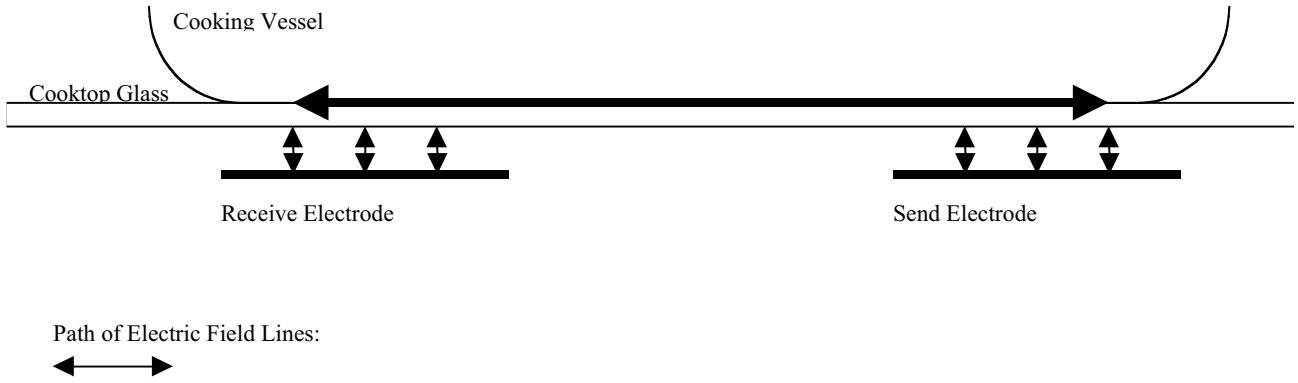

Figure 1: Basic Transmit/Receive Mode Pot Detector

Tested Configuration

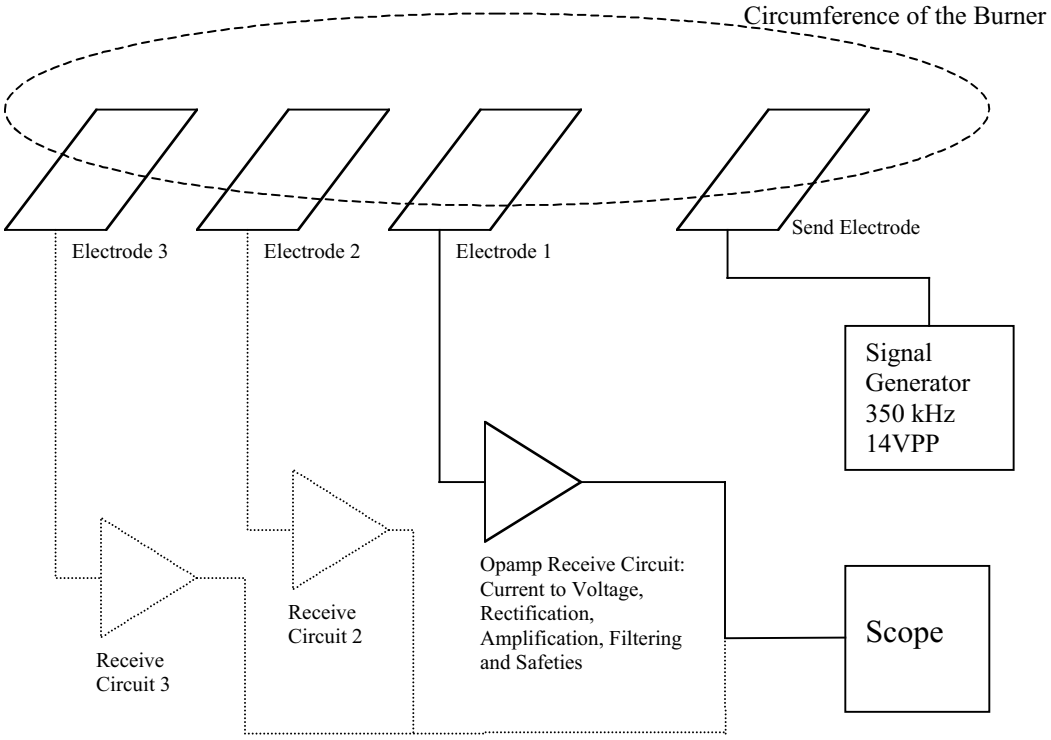

Figure 2: Multi-electrode Transmit/Receive Mode Pot Detector

Circuits:

The send electrode was driven by a signal generator running a sine wave at 350 kHz, 14VPP. This frequency gave better sensitivity than lower frequencies, because of the larger amount of capacitive coupling. It is possible that higher speed OpAmps would permit frequencies that are higher still and therefore allow for even more sensitivity. Increased sensitivity allows for smaller electrodes, greater distances between the electrodes, and simpler analogue to digital back ends. Raising the voltage also increased sensitivity. More amplification stages would also give greater sensitivity.

Each of the receive electrodes was attached to opamp circuitry that converted current from the electrode to a voltage, and then followed this with rectification, amplification, and filtering stages. This device essentially used three receive channels of Lance Borque's capacitive detection circuit, as described in the section of this report that discusses the slider. The signals from the receive circuits fed into a scope for simple monitoring.

Testing

Four pots and pans were placed on the surface of the glass over the burner. Pots of different makes and compositions were tried. Their placement along the primary axis of the electrode row was varied.

Results and Conclusion

The results of the test were solid. There was more than enough sensitivity to allow for more, smaller, and differently spaced electrodes. Most pots caused a 1 volt signal to the scope when placed over any particular send and receive electrodes. When not directly over both electrodes, but near them, a smaller signal was seen at the scope. This meant the electrode configuration permitted information about the size and location of pots on the cooktop surface to be inferred from the scope readouts. There is an effect, however, when the pot is contacted. Although this inhibits the system from working properly when the pot is touched, the signal is quite dramatic, however and seems able to be distinguished from other situations easily, potentially giving additional information (e.,g., the user is touching the pot or stirring the pot with a conductive stirrer).

Other geometries could be promising. For example, several pairs of send receive electrodes circling the burner heat shield may be able to infer quite accurately the size and location of pots on the burner. Many configurations over the burner could also give good results, but they must be able to withstand the high temperatures present inside the heat shield.

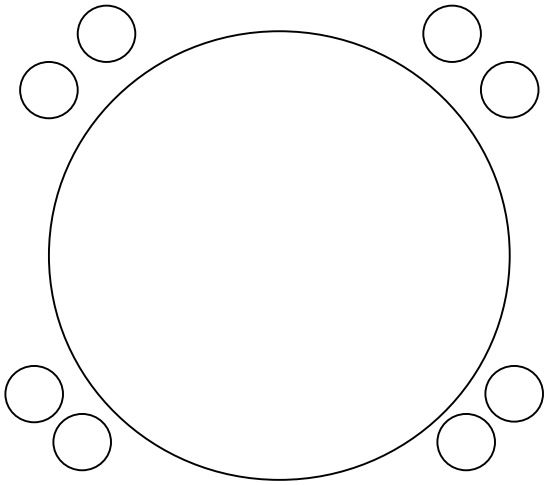

Figure 3: Multi-electrode Transmit/Receive Mode Pot Detector

A separate, four burner capacitive loading-mode system using a multichannel Motorola capacitive sensing chip (the MC33794) was constructed and showed some promise. It is another route which could be pursued. However, it does not appear to be as flexible as the send-receive method, and the signals were marginal.

Inferring Glass Ceramic Temperature by Detecting Low Wavelength Infrared Light Leaking from the Edge

Philip Bramsen and Hong Ma
Responsive Environments Group
MIT Media Lab

Abstract

To measure the temperature of glass used to cover cooktops, a narrowband photoconductive detector paired with a blindfolded detector (for compensation of local thermal effects) was used to pick up the infrared light emitted by the heated glass and infer the glass temperature. Rather than mount the photodiodes above the cooktop looking down, they were mounted at the edge of the glass ceramic, where they looked through the glass towards the region of the glass above the burner. This makes a compact assembly that doesn't need cleaning, and always guarantees that the glass ceramic surface is being measured.

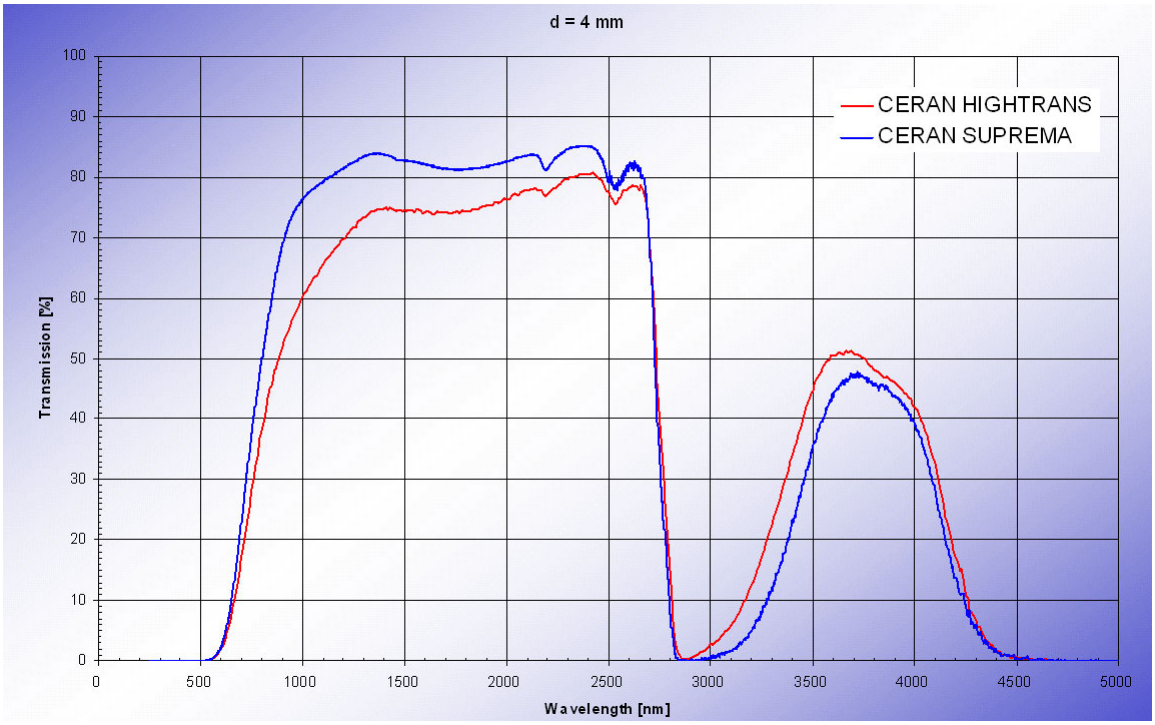

Figure 1: Optical transmission through Schott Glass Ceramic

Concept and Introduction

Depending on temperature, the glass emits light in 1 to 5 μm range when heated. Internal reflection and direct transmission carry the light through the plane of the glass, which is roughly 80% transparent between 1.3 and 2.7 microns of wavelength (see Fig. 1

above). A well-placed photosensitive detector could pick up this light. The resulting signal would have a correlation to the temperature of the heated glass, as with a modern IR thermometer. However, actual heating of the glass in the region of any sensors, as well as low transmission levels through the glass, radiant heat, and light from windows or certain lamps can all interfere with attempts to focus in on the specific range of IR which is related to temperature.

Therefore, a PbS photoconductive detector with a specific spectral response was chosen. In addition, a circuit allowing for a thermally linked second photodiode for temperature compensation was designed. Eliminating the effects from light sources outside the glass and forcing controlled, even warming of the photodetectors was accomplished by careful shielding of the photodetectors.

Design and Construction

The first stage is a pair of photocsensors feeding into a differential opamp chosen for the application. One of the photosensors is blindfolded; it sees no light, but is in every other way mounted to the glass just as the seeing sensor is. This allows for good compensation for inaccuracies caused by changes in temperature of the seeing photosensor. An alternative method for compensation or a method for further compensating the circuit for temperature fluctuations would be to add a thermistor.

Following the differential amplifier are a low pass filter and an amplification stage. As tested, this circuit feeds into a scope, but could be adapted for an analogue to digital converter and microprocessor.

The circuit drew power from a +/-12V power supply. Two regulator circuits onboard with the opamps permit a range of supply voltages.

Photodetector:

The Hamamatsu P394 fit the application well. It has a good spectral response to match the emissions of the glass and does not behave erratically when warmed.

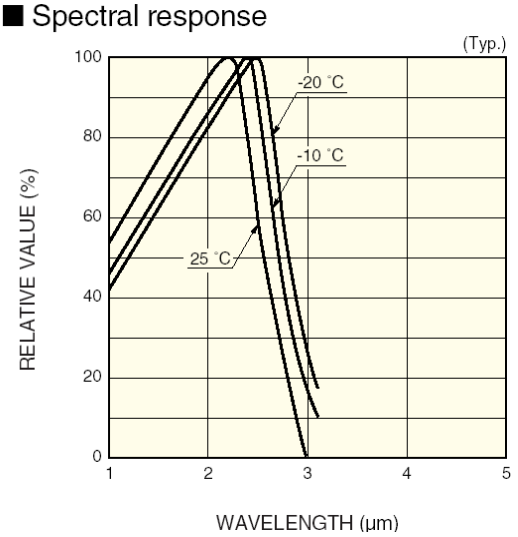

Figure 2: Spectral Response of the Hamamatsu P394

Circuit:

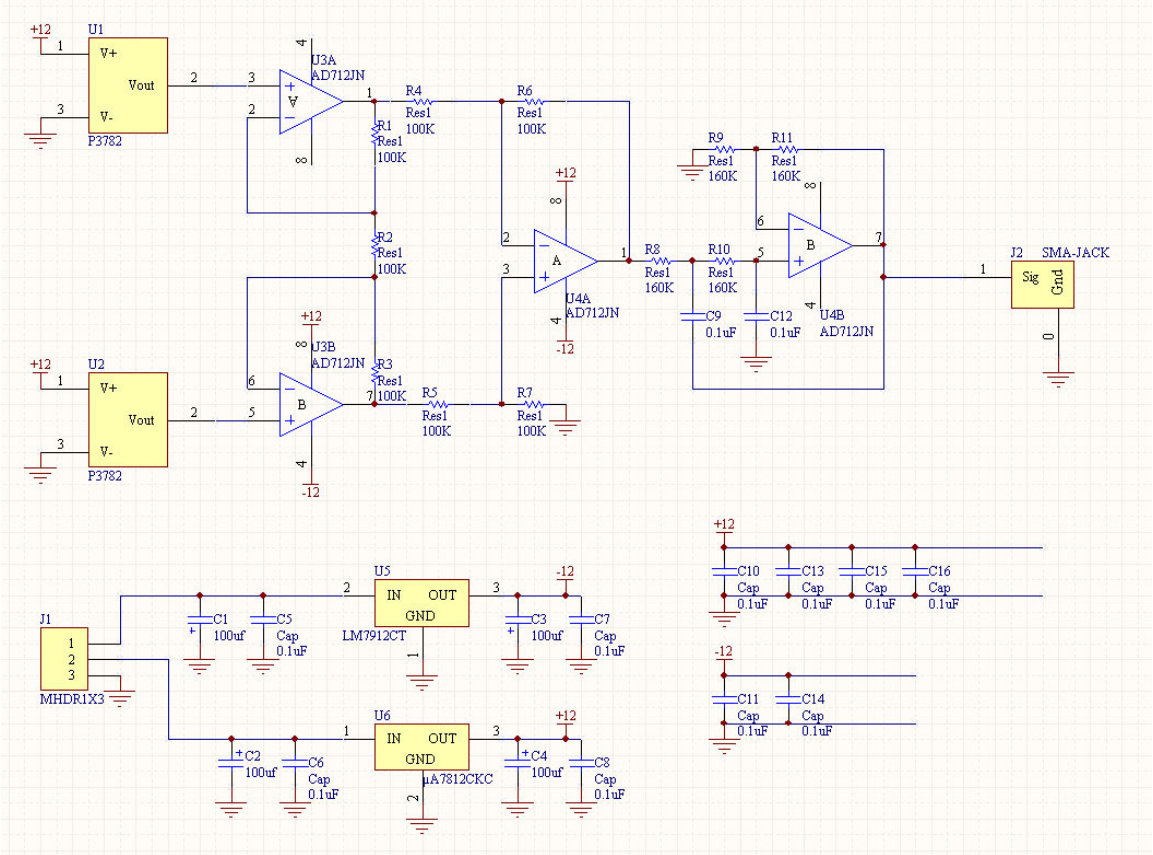

Figure 3: Schematic showing Electronics for Conditioning Photodetector Signals

Mounting:

It is critical that the sensor sees only the edge of the glass. Even a small quantity of sunlight or light from halogen lamps caused reactions in the sensor equivalent to what we would expect from changes of 200 degrees Fahrenheit. As track lighting common in kitchens uses halogen lamps, good shielding and optical contact to the edge of the glass is critical.

For proper operation of the differential opamp to eliminate the affects of warming the sensor, identical mountings for both sensors as well as thermal contact between the sensors is important. Accordingly, the photodiodes were joined to the glass with optical grease that was transparent at these wavelengths, the two photodiodes were thermally coupled with thermally conductive silicone paste, and copper tape shielded all ambient illumination not coming through the glass. Figure 4 shows the electronics mated to the edge of the glass ceramic test piece, illustrating these precautions.

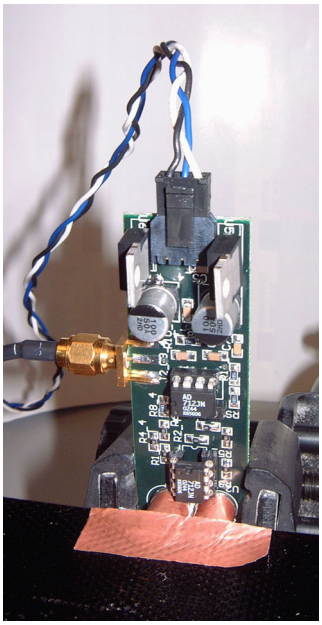

Figure 3: Electronics Board, with Photodiodes Mounted at the Edge of the Glass Ceramic

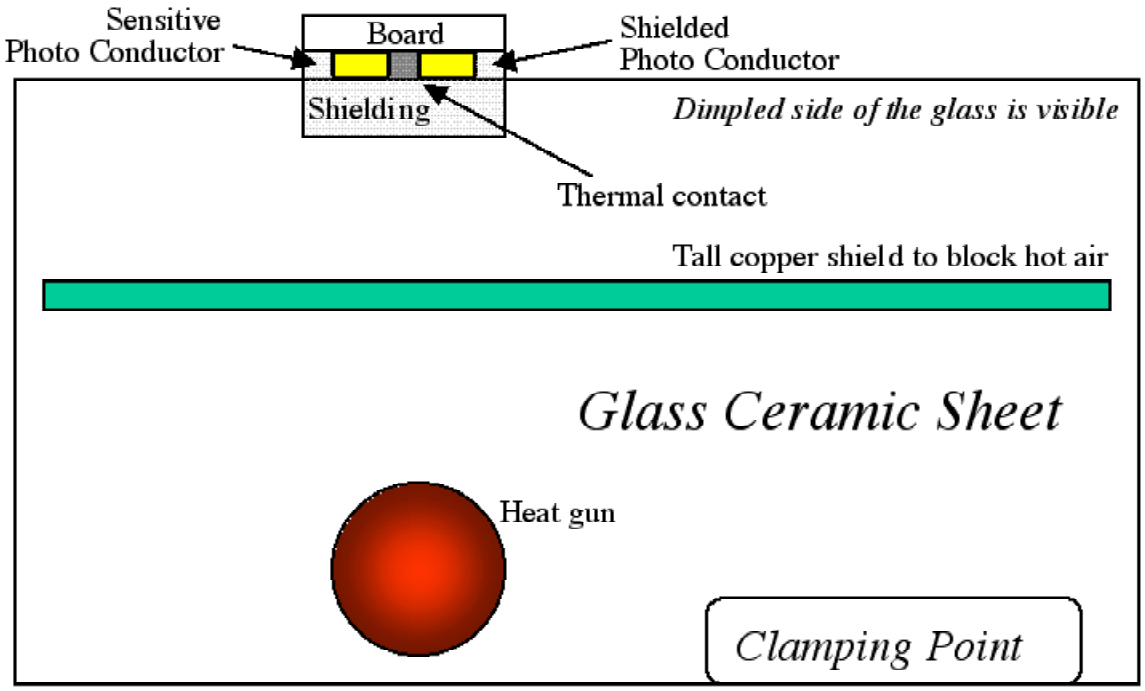

Figure 4: Test Rig, showing placement of all elements and heat application

Testing

The glass was heated to roughly 600 degrees Fahrenheit with a heat gun. Greater temperatures were not attempted, as 600 degrees caused the glass to smoke, presumably because the heat gun also adds currents of hot air and can burn any residual material on the glass, and thereby encourages the smoking. The same hot air required a large thermal shield to protect the circuit from heating up, as warming upset the circuit reading. Further design should take this into consideration.

As the glass cooled, more than 15 data points were taken, each point having both a voltage from the circuit with respect to a reference voltage and a temperature reading from an industrial grade thermocouple thermometer. Scope levels from the circuit and the thermocouple permitted monitoring of the stability of the temperature reading and comparisons with the circuit output for qualitative observation of the smoothness and monotonic operation of the sensor circuit.

Since the glass cools rapidly at first and the distribution of the heat in the glass changes quickly when the heat gun is no longer holding the temperature high, data for the first hundred degrees of change was not taken, but the scope implied smooth, monotonic behavior.

Spot heating with a small butane torch proved to be inadequate because a large enough region could not be easily heated. Removing the torch permitted very rapid dissipation of the heat through the plane of the glass from the spot heated by the torch. This resulted in the photoconductive detector picking up much less from the “bright spot” heated by the torch, even though the thermometer showed that all but the bright spot remained nearly at the temperature maintained when the torch was present. A rapid decay in output from the sensor circuit appeared to indicate the glass was cooling faster than the thermometer suggested. The thermometer had a long time delay caused by slow cooling. This meant that the thermometer warmed internally, and then lagged the photodetector. Therefore, for reasons due to the overwhelming affects of heat dissipation through the glass and heating of the thermometer, watching rapid cooling proved to be impractical.

However, observation showed that the early cooling when the heat gun was used and the cooling that resulted when the torch was used were the same. This implies that just as the problems caused by heating with the small torch were overcome by using a heat gun, a heat source superior to the heat gun would probably extend the testable range of the sensor.

Results

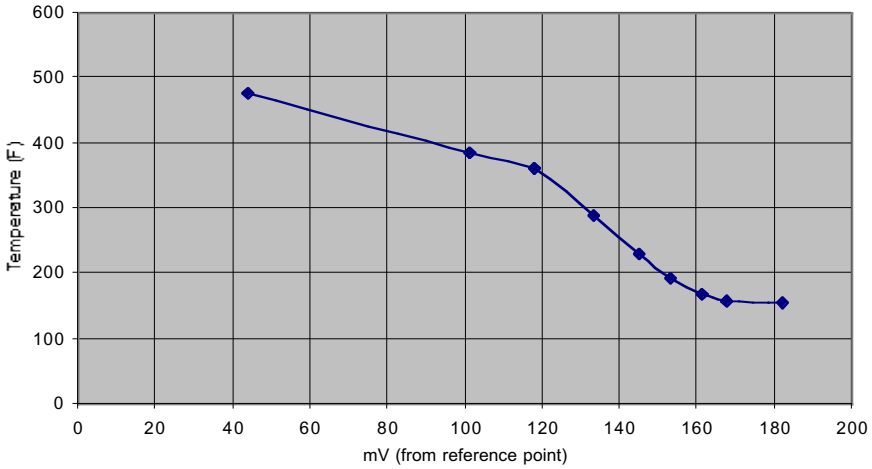

Figure 5: Temperature (°F) vs. mV (from reference point) - Combined Data

The early data was taken as the glass cooled quickly, this makes it less precise. Also, the early data was taken while the probe was held on the glass for longer than is ideal. The probe heats and then lags the actual rate of cooling of the glass. Furthermore, the bumpy surface of the glass caused additional imprecision. Nevertheless, the results suggest a strong, smooth correlation to temperature. And noting that some of the problems were proven to be from the thermometer suggests that IR detection could be superior to a surface mounted thermometer.

It should be noted that when the scope was watching a time elapse decay of the temperature and circuit output, the results were fully monotonic and smooth for the entire range observed.

Analysis

The roughly linear behavior of the output of the sensor circuitry suggests that a simple correlation of the IR emissions to the glass temperature was present.

Problems such as warmed sensors, ambient light, and low transmission levels through the glass were all solved, at least in this test rig. However, high temperatures have not been fully explored, and applying this system in an actual cooktop would involve careful design to eliminate effects from photodetector heating. One must also keep in mind that because of the residual 20% absorption in the glass ceramic, there will be a calibration change as the heated spot moves away from the photodetectors.

Piezoelectric Transducers and Schott Ceran Glass Ceramic

Mateusz Malinowski

July 15, 2003

Abstract

The following report summarizes an examination of the applicability of piezoelectric transducers to temperature measurements of Schott Ceran glass ceramic. Though the measurement is coarse, techniques were developed to improve the resolution. The sensors were further used to detect the presence of cookware and liquid spills on the glass ceramic cooktop, with limited success.

1 Experimental Setup

Piezoelectric ceramic transducers provide a convenient way for converting electrical energy to mechanical and vice-versa, and have found numerous applications in sensing, non-destructive testing, and sound generation. In the present experiment, two piezoelectric transducers were employed (one as a transmitter, the other as a receiver) to send ultrasonic vibrations across a 50 cm × 15 cm piece of glass ceramic, used to simulate the area of a glass ceramic cooktop around a burner. To conduct temperature-response measurements, the glass was heated from above with a hot-air gun or placed above an electric burner and heated from below.

The two PZT (Lead Zirconate Titanate) piezoelectric ceramic transducers were separated by 30 cm, as they would be when measuring the temperature above a burner, and bonded to the glass with two-part epoxy adhesive. Leads were soldered to the top and bottom of the transducers. The transmitter (on the left in Figure 1) measured 7.3 cm × 1.4 cm. The longer side is perpendicular to the direction of sound propagation in order to ensure a narrower beam and fewer reflections. The receiver (measuring 3 cm × 1.3 cm) is oriented with longer side in the direction of sound propagation, resulting in more force on the transducer and better reception.

The transmitter was driven directly by a function generator via leads soldered to the top and bottom electrodes. Similar electrical connections were made with the receiver. The output was first sent directly to an oscilloscope, but an active high-pass filter cascaded with a state-variable bandpass filter (see schematic in Figure 3) was later utilized to amplify the signal and eliminate noise due to environmental disturbances.

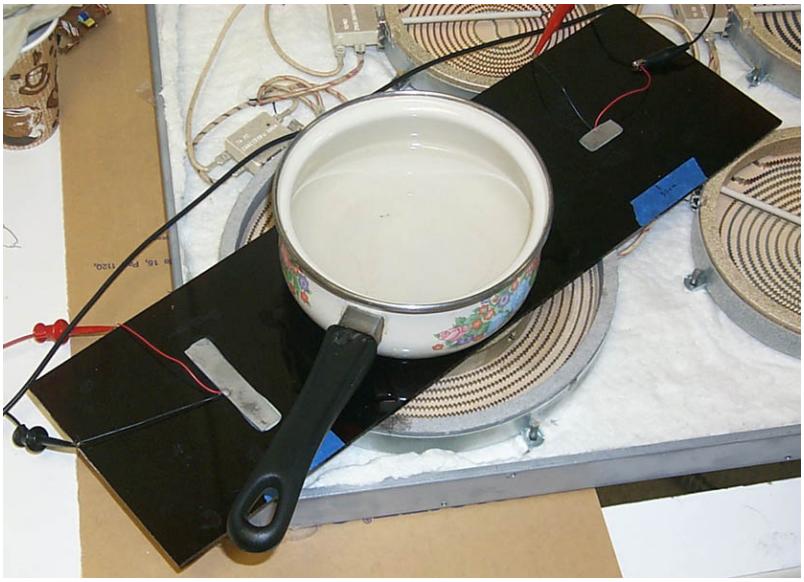

Figure 1: Photograph of experimental setup. The transmitter is on the left, while the receiver is on the right.

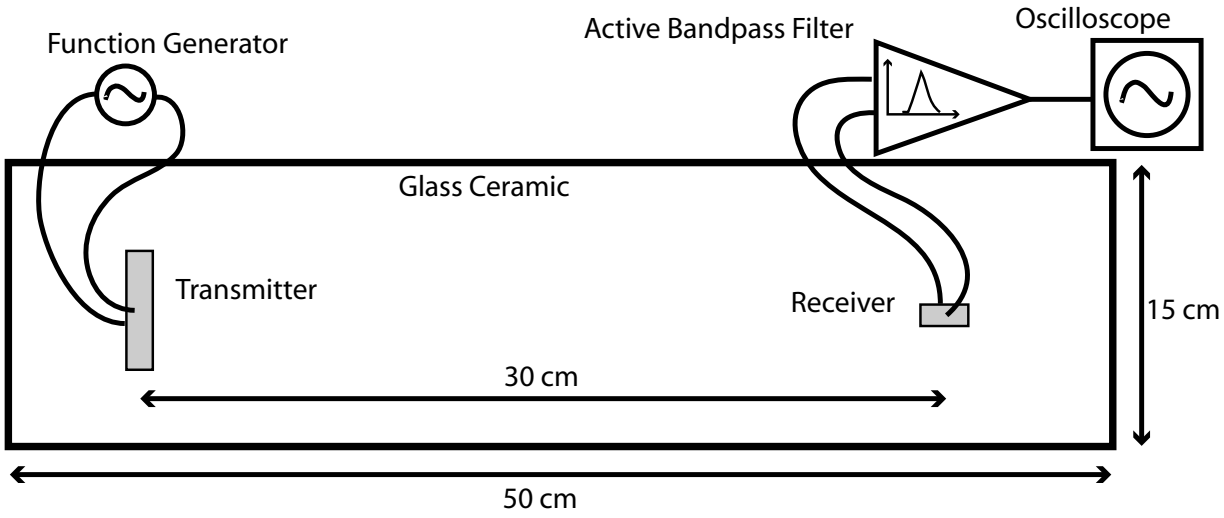

Figure 2: Schematic diagram of the experimental setup.

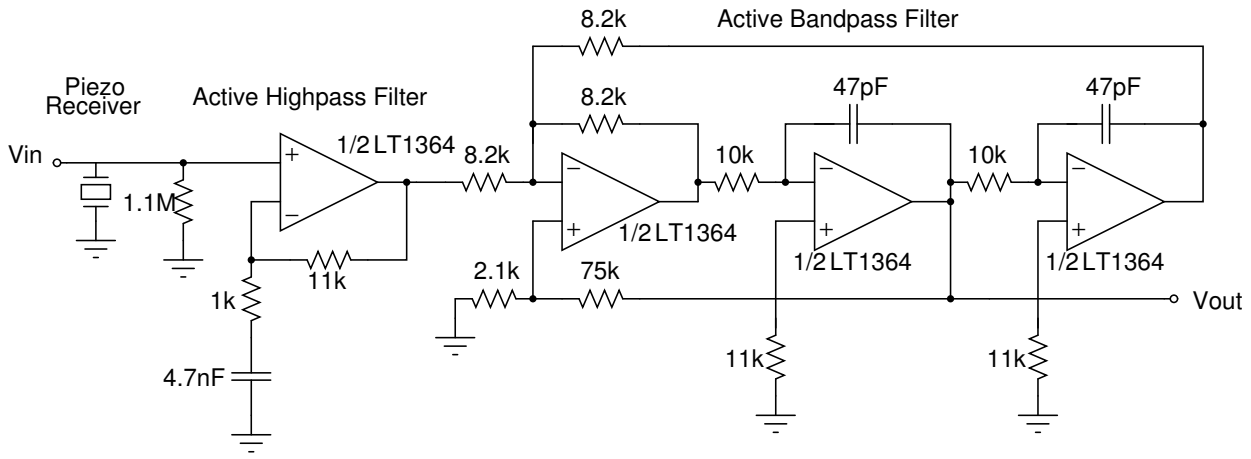

Figure 3: State-variable bandpass filter with center frequency around 300 kHz and a gain of 10. The input stage is an active high-pass filter with bandwidth of 40kHz and a further gain of 10.

2 Temperature Measurements

2.1 Time Delay

The speed of vibrations through a material is a function of density, Young's modulus, and Poisson ratio. These mechanical properties will change depending on the temperature, slowing vibrations with increasing temperature.

The velocity can be measured by timing the propagation delay across the burner, from one transducer to the other. To conduct this measurement, multi-count bursts of ultrasonic sine waves were sent to the transmitter; a delayed signal, together with distortions, reflections, and dispersions was read at the receiver. The input and room-temperature output signals are portrayed in Figure 4.

As can be seen in Figure 4, there are numerous wave packets at the output. Their numbers can be attributed to reflections off the edges of the glass as well as to the fact that the glass ceramic supports different kinds of vibrations, which travel at different speeds. In addition to sub-surface longitudinal waves, the primary method of sound propagation, the transmitter induces sub-surface transverse waves (shear waves) as well as Rayleigh waves (also known as surface acoustic waves or SAW) which only travel near the surface.

At room temperature Schott Ceran glass ceramic has the following mechanical properties [2]:

$$\begin{aligned} \text{Density} &: \rho = 2.6 \times 10^3\,\text{kg/m}^3 \\ \text{Young's Modulus} &: Y = 95\,\text{GPa} \\ \text{Poisson Ratio} &: \nu = 0.25. \end{aligned}$$

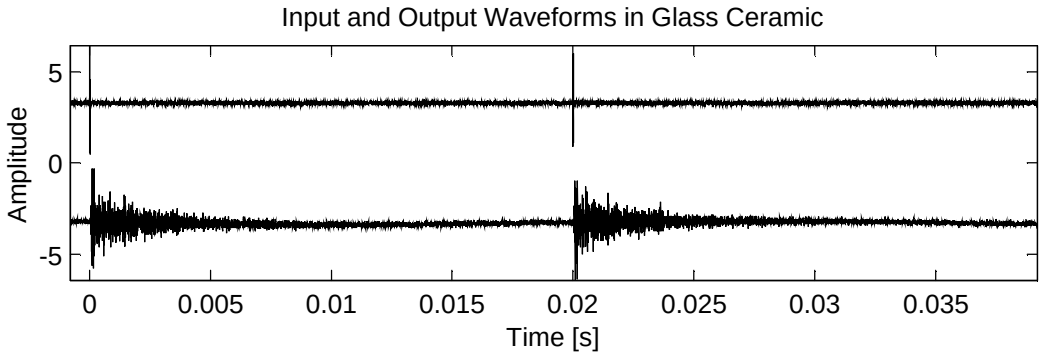

(a) Large time scale.

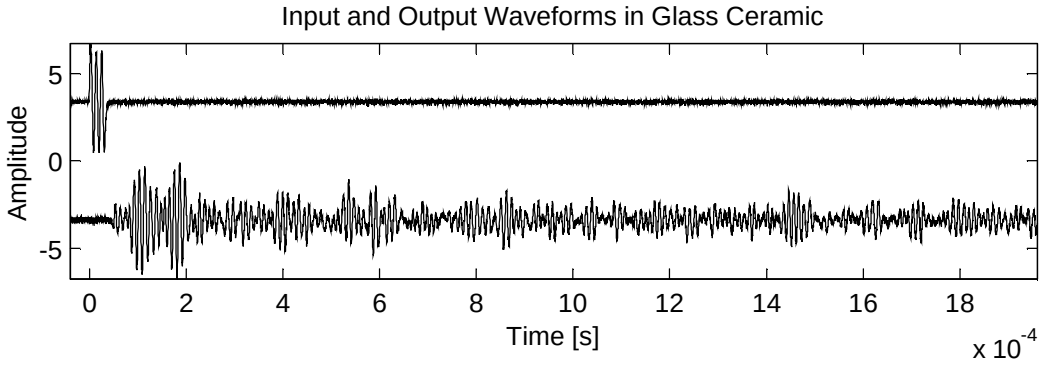

(b) Medium time scale.

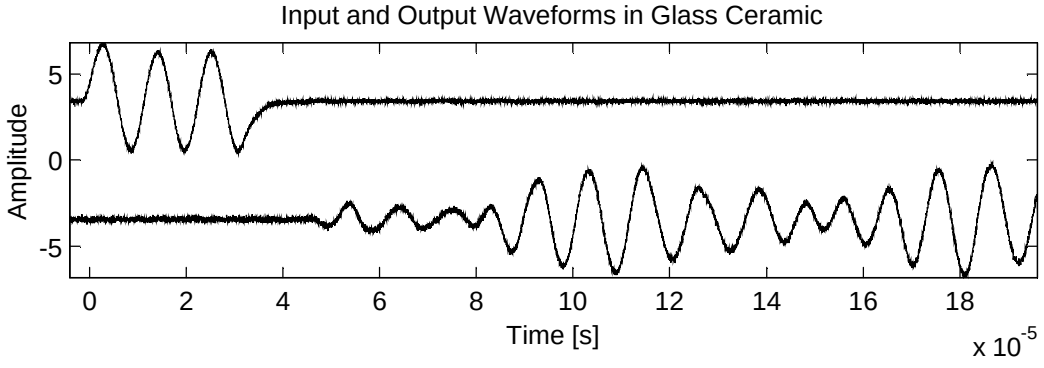

(c) Small time scale.

Figure 4: Input and output waveforms; 3-count 180kHz waves at 21° C

Given the above, longitudinal waves should have a velocity of 6621 m/s.

$$\begin{aligned} c_L &= \sqrt{\frac{Y(1-\nu)}{\rho(1+\nu)(1-2\nu)}} \quad [1] \\ &= \sqrt{\frac{9.5\times10^{10}\,\mathrm{N/m^2}(1-0.25)}{2.6\times10^{3}\,\mathrm{kg/m^3}(1+0.25)(1-0.5)}} \\ &= \sqrt{\frac{7.125\times10^{10}\,\mathrm{kg/s^2m^2}}{1.625\times10^{3}\,\mathrm{kg/m^3}}} \\ &= 6621\,\mathrm{m/s} \end{aligned}$$

The velocity of transverse vibrations can be calculated as follows [4]:

$$\begin{aligned} c_T &= \sqrt{\frac{E}{2\rho(1+\nu)}} \\ &= \sqrt{\frac{9.5\times10^{10}\,\mathrm{N/m^2}}{2(2.6\times10^{3}\,\mathrm{kg/m^3})(1+0.25)}} \\ &= \sqrt{\frac{9.5\times10^{10}\,\mathrm{N/m^2}}{6.5\times10^{3}\,\mathrm{kg/m^3}}} \\ &= 3823\,\mathrm{m/s} \end{aligned}$$

Given the two velocities, it is possible to calculate the Rayleigh wave velocity using the following two relations [4]:

$$4\left(\frac{c_T}{c_R}\right)^2\sqrt{1-\left(\frac{c_T}{c_R}\right)^2}\sqrt{\left(\frac{c_T}{c_L}\right)^2-\left(\frac{c_T}{c_R}\right)^2}+\left[1-2\left(\frac{c_T}{c_R}\right)^2\right]^2=0 \quad \text{and} \quad c_L>c_T>c_R>0$$

The resultant velocity is $c_R = 3515\,\mathrm{m/s}$. Since the longitudinal waves are fastest, their effects dominate, and they will be the focus of the study.

Since the longitudinal wave velocity is 6621 m/s, the first packet should arrive at the transducer after time $t_d = \frac{0.3\,\mathrm{m}}{6621\,\mathrm{m/s}} = 45.3\,\mu\mathrm{s}$. This is confirmed by looking at the receiver output in Figure 4(c).

Unfortunately, the dependence on temperature of the longitudinal velocity (and therefore the time delay) is weak. The coefficient of linear expansion is $\alpha = 3.2\times10^{-6}\,1/\mathrm{C}^\circ$; for a change in temperature of $100\,\mathrm{C}^\circ$ the density will increase by a factor of $(1+3.2\times10^{-4})^3$ or 1.001. This will—assuming Young's modulus and Poisson ratio are independent of temperature[1]—slow the longitudinal vibrations to 6618 m/s and extend the delay by $\Delta t_d \approx 20\,\mathrm{ns}$. Even if the above assumption is incorrect (i.e. Young's modulus and Poisson ratio *do*

[1] An analysis of the temperature dependence of Young's modulus in normal glass shows it to be weak in the range of working temperatures [3]. Likewise, the Poisson ratio for most materials remains constant up to a certain temperature at which the material deforms. In the case of Ceran glass ceramic this temperature is greater than 500°C, beyond the working range of the stove.

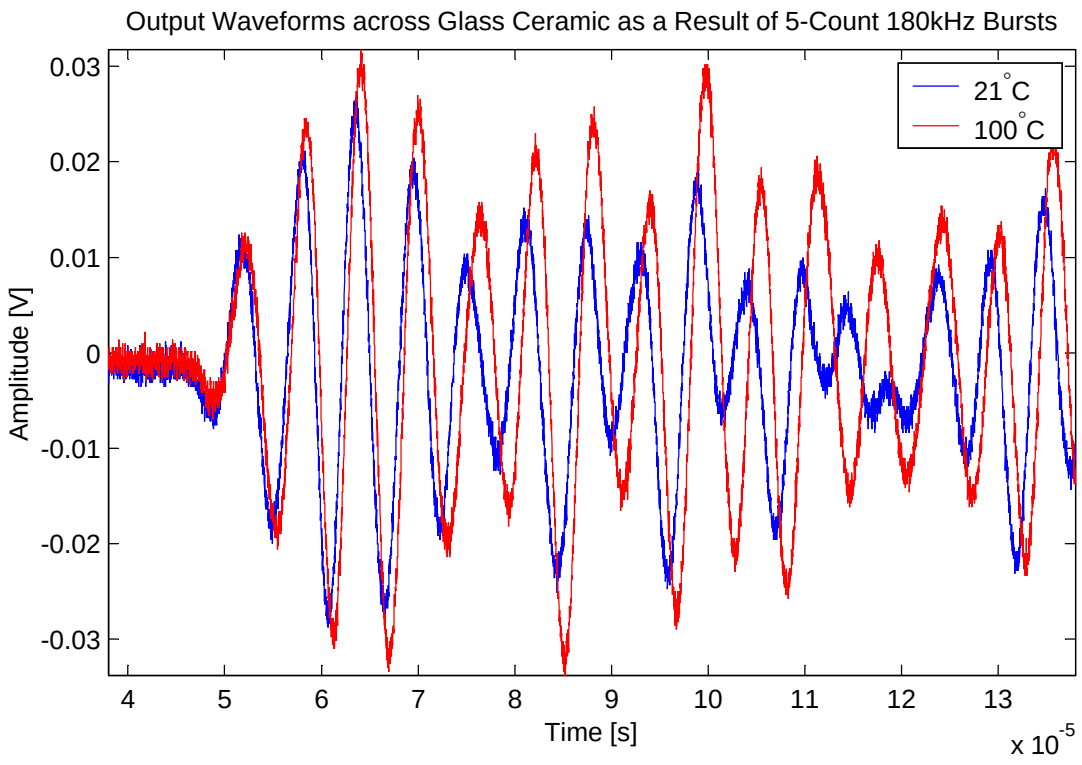

Figure 5: Output waveforms at different temperatures. There is no discernible arrival time delay difference at different temperatures.

change with temperature), the change in the arrival delay is imperceptible, as Figure 5 demonstrates.

2.2 Interference Delay

There is, however, a marked difference between the output waveforms at different temperatures. Furthermore, the differences become more accentuated at higher frequencies, as can be seen in Figure 6. While the time delay described above is on the order than 20 ns per 100 C°, the effect seen in Figure 6 is on the order of 200 ns or more.

The scale of the temperature dependence can be attributed to interference and superposition of wave packets, as vibrations take different paths through the glass from transmitter to receiver. Even at room temperature, one can see a beating pattern, characteristic of the superposition of two waves of slightly different wavelength. This behavior can be derived as follows, where y_1 and y_2 are the two waves being superposed (assumed for simplicity to have unity amplitude):

$$\begin{aligned} y &= y_1 + y_2 \\ &= \sin\left(\frac{2\pi}{\lambda_1}x\right) + \sin\left(\frac{2\pi}{\lambda_2}x\right) \end{aligned}$$

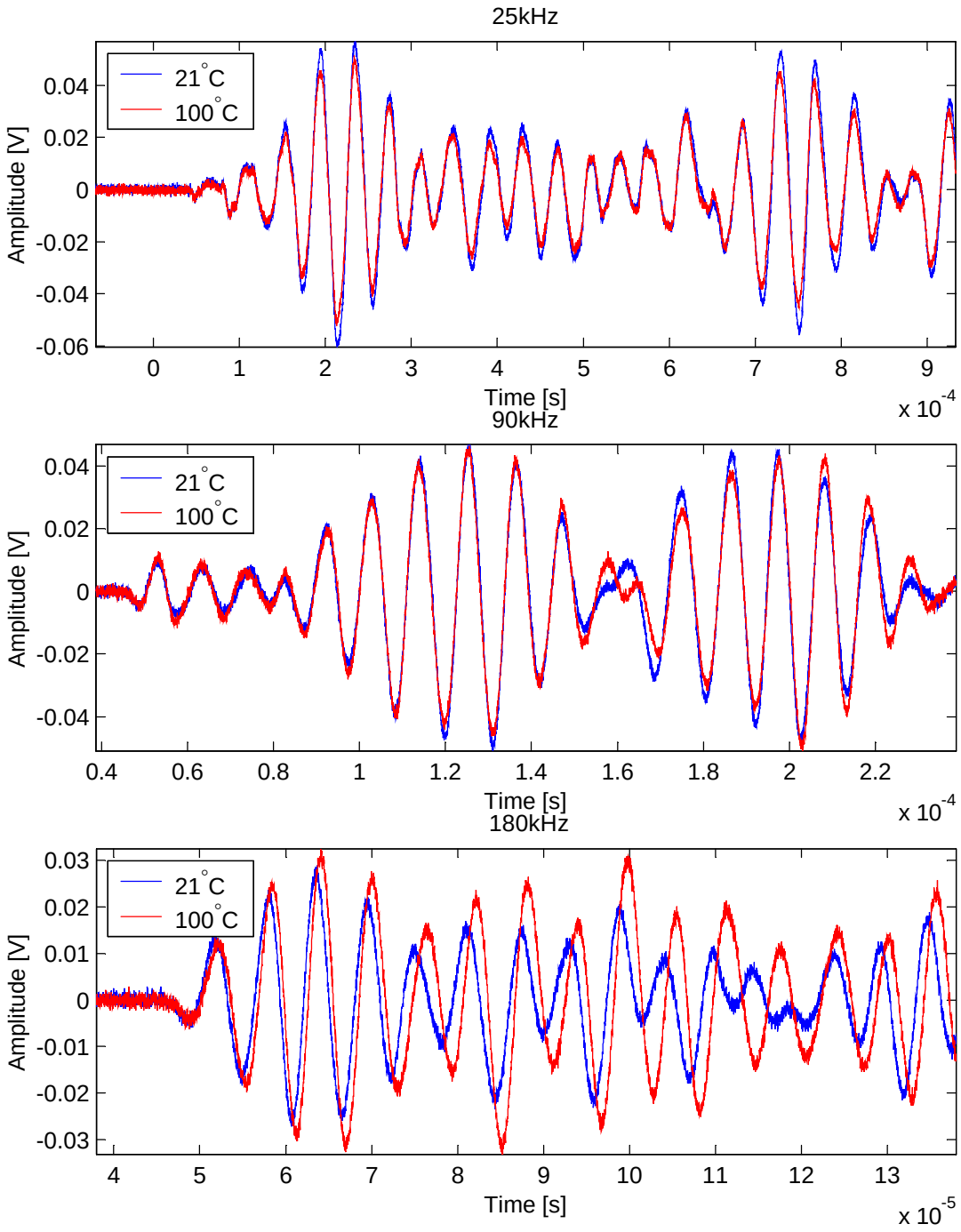

Figure 6: The interference delay effect which depends on temperature becomes more noticeable at higher frequencies.

$$
\begin{aligned}
&= \sin(2\pi k_1 x) + \sin(2\pi k_2 x)\,,\ k = \frac{1}{\lambda} \\
&= 2\sin\left(2\pi\frac{k_1+k_2}{2}x\right)\cos\left(2\pi\frac{k_1-k_2}{2}x\right)
\end{aligned}
$$

The resultant wave is composed of one similar to the original two (the sine term), whose wave number k is the mean of the original two, modulated by another (the cosine), which if $\lambda_1 \approx \lambda_2$, will be much lower in frequency, acting as a modulation envelope for the higher-frequency sine wave.

In this case, the difference in wavelength that causes the beating is due to the hot glass slowing down the vibrations, more or less, depending on the path taken. The pattern produced by this superposition is very sensitive to its constituent waveforms, and a slight delay in one of the original waveforms can produce a large shift in the sum.

The exact origin of the superposition—i.e. which waves are being superposed—is not clear. The small size of the glass ceramic used in the experiment leads to various reflections that are hard to track. This, compounded with a variety of vibration modes within the glass makes it difficult to determine which reflections are responsible for the beating pattern.

Since the first superposed "beat" arrives at the receiver roughly $10\,\mu$s after the first vibration, this corresponds to an additional path length of 6.6 cm, given that the relevant vibrations propagate at a speed of 6621 m/s. This longer path length could be due to a reflection off the side of the glass. A full-scale implementation would clarify this issue, as the edges of the glass would be farther away. Furthermore, this sort of interference could be controlled in a full-scale implementation by using two receivers at the same distance from the transmitter. One would receive vibrations from across the burner, while the other would act as a control, receiving its signal through the cooler glass between the burners.

As it stands, however, there is a definite relationship between the interference shifts and temperature (see, for example Figure 7). Secondly, as the velocity due to temperature decreases and the wavelength increases, the beating increases in frequency, meaning that the output waveforms at various temperatures differ by both phase and amplitude. If one takes the room-temperature output waveform as reference, the waveforms at higher and higher temperatures will become less correlated. If one takes the root-mean-squared value of the correlation, and plots it against temperature, the relationship becomes quite clear, as can be seen in Figure 8.

As mentioned earlier, it is difficult to determine the origin of these effects. It is possible that the delays and changes in amplitude are not at all due to the changing temperature of the glass, but are instead due to the inadvertent warming of the piezo receiver. When heated with a hot-air gun to a temperature of 100 °C, the glass ceramic sample conducts well enough that the receiver temperature reaches 40 °C. To investigate

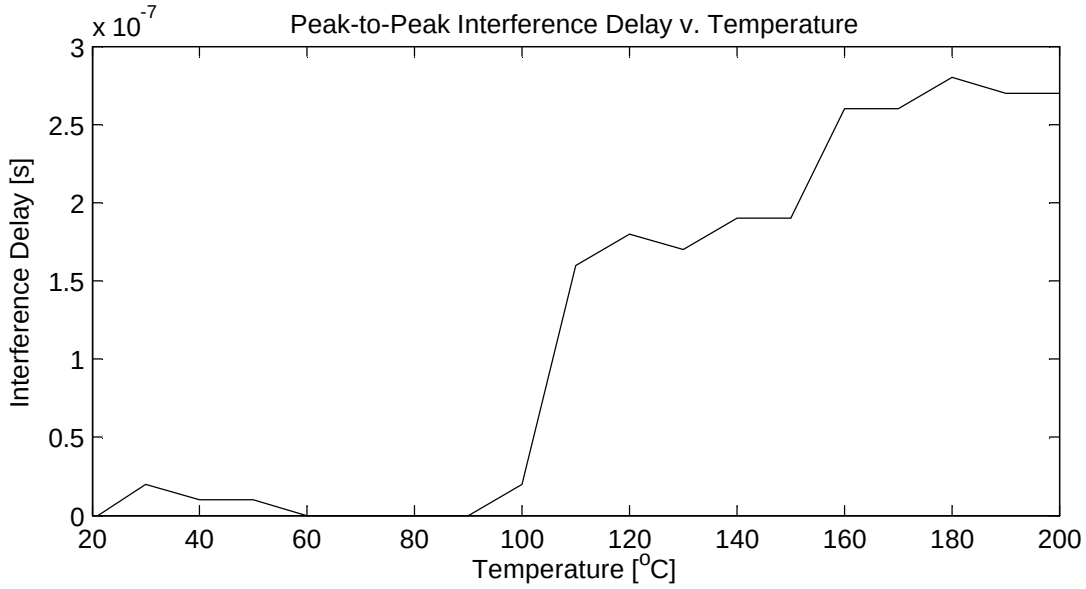

Figure 7: The position of the highest peak in the center of the first beat is measurably affected by temperature.

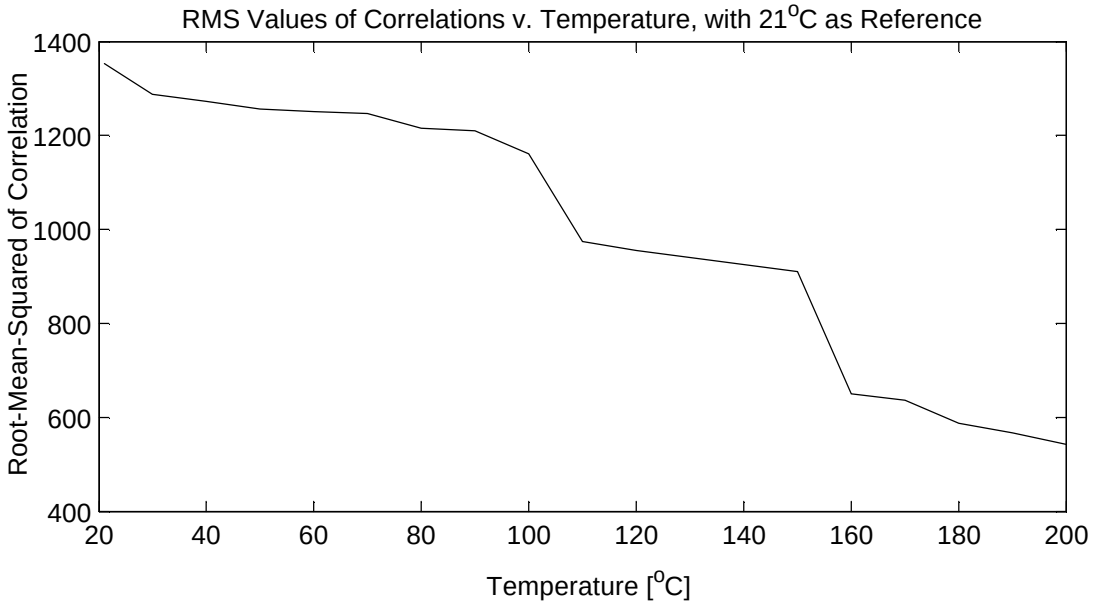

Figure 8: Output waveforms at higher temperatures become progressively less correlated to the 21 °C reference waveform.

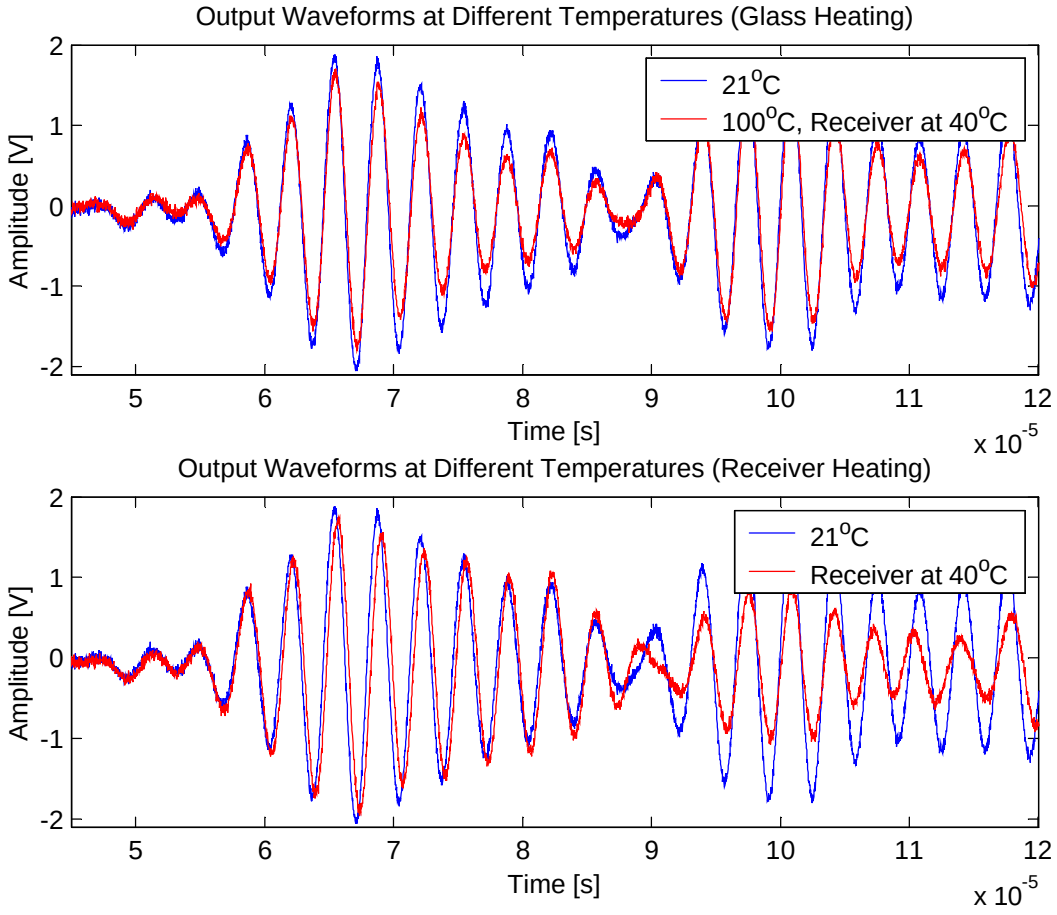

Figure 9: As the piezo receiver heats up, it alters the output waveform, independent of the temperature of the glass ceramic.

the effect of this collateral heating, the receiver was heated to 40 °C, while keeping the glass cool. These results were contrasted against the standard 21-/100-degree curves. As Figure 9 demonstrates, there is a noticeable effect, with the amplitude dropping off drastically as the temperature increases.

While this phenomenon has not yet been studied at-length, it points to some limitations of using piezoelectric transducers to measure temperature. On the other hand, using a burner as opposed to a hot-air gun, would ensure some more control over heat propagation.

3 Pot Detection

As the majority of vibrations detected by the receiver are internally-propagating transverse waves, surface loading due to pots and other cookware shows no effect on the output, as can be seen in Figure 10, where output waveforms for a loaded and unloaded piece of Ceran glass ceramic are indistinguishable.

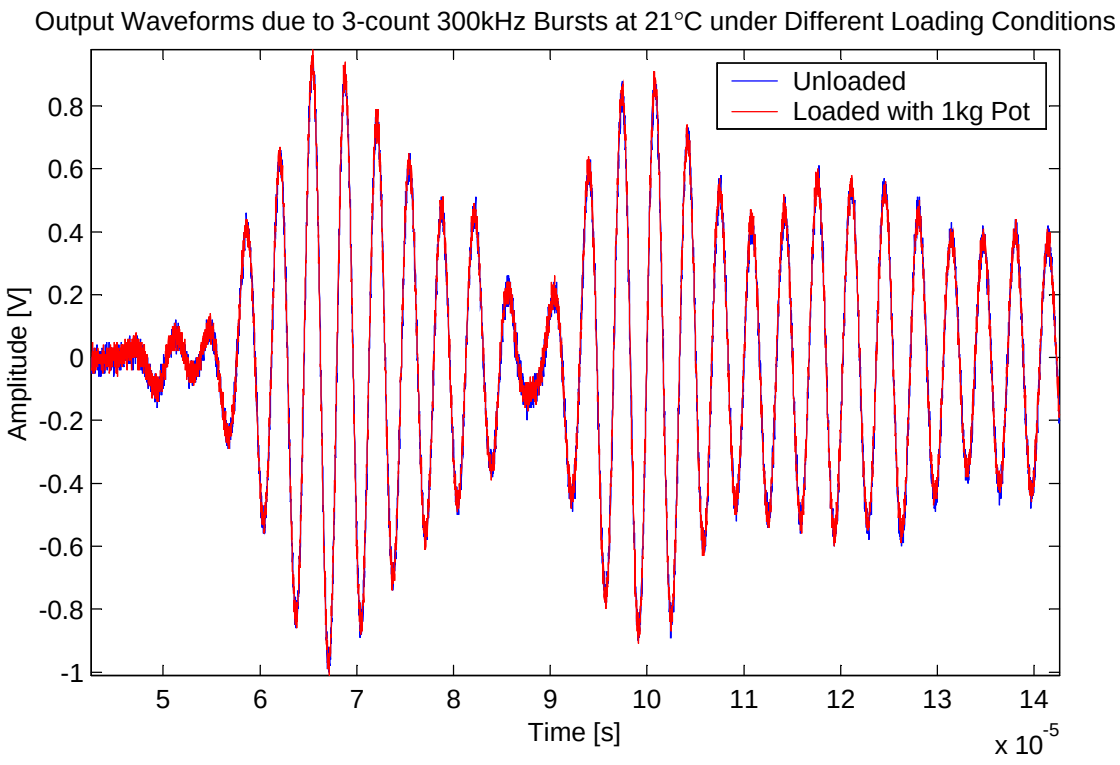

Figure 10: The loading of the glass ceramic surface by cookware has no effect on the output waveforms.

While this result proves piezoelectric transducers useless for pot detection, it does make any other measurement applications more robust as the output will remain consistent, no matter what the load on the cooktop surface.

4 Spill Detection

While metallic cookware seems to have no effect on the propagation of ultrasound through the glass, liquid spills do have an effect. The output waveforms of vibrations propagating through wet glass differ significantly from those associated with dry glass. Figure 11 shows that the two waveforms differ in peak amplitudes and general shape, furthermore, there is a noticeable delay between the two.

5 Other Applications

In addition to the active uses of the experimental setup there are possible other passive uses. These would require just one piezoelectric transducer as a receiver, with the environment providing the inputs. A possible application of such a passive system would be a boil detector. Continued vibrations at a specified range of

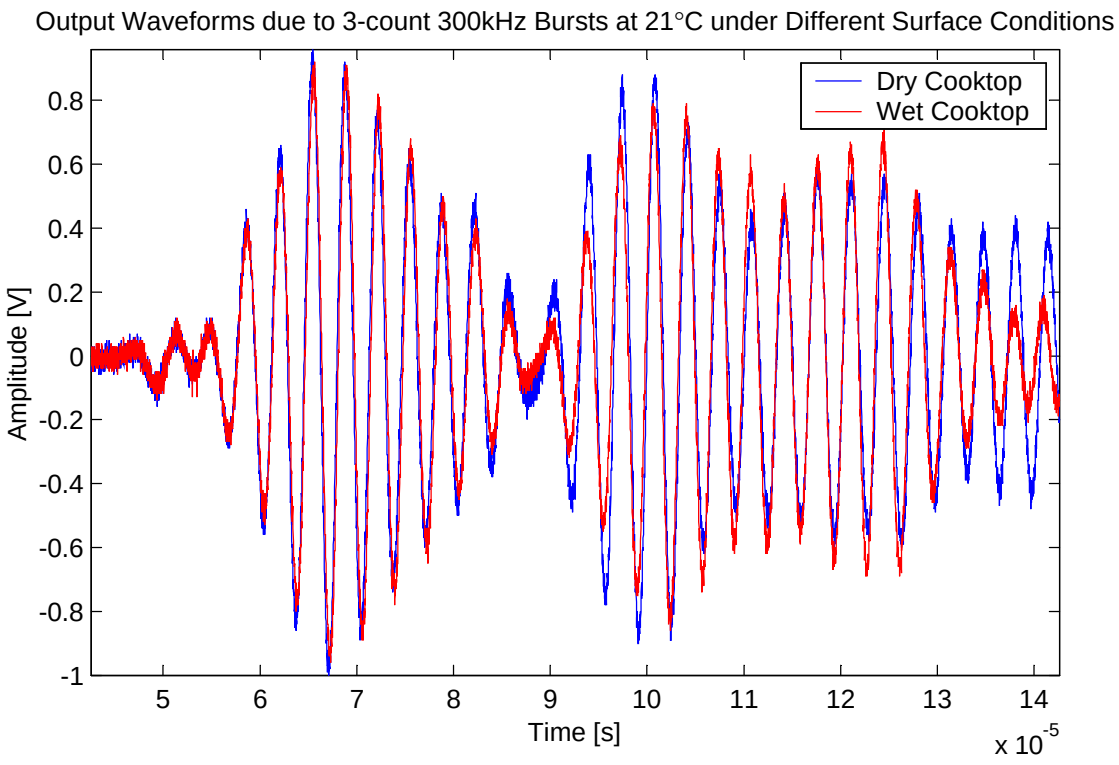

Figure 11: Liquid spills greatly affect vibrations propagating across glass ceramic.

frequencies could indicate that the water is ready.

References

[1] Jacob Fraden. *Handbook of Modern Sensors*. Springer Verlag, 2nd edition, 1997.

[2] Schott. Ceran product handbook: Product properties. Technical Report TL 1001-01, Schott, 2001.

[3] A.I. Shutov and I.V. Lakmetkin. Approximation of temperature dependence of the modulus of elasticity of glass. *Glass and Ceramics*, 55(11–12):368–369, 1998.

[4] H. Überall. *Surface Waves in Acoustics*, volume 10 of *Physical Acoustics: Principles and Methods*, chapter 1, pages 3–4. Academic Press, 1982.

Difficulties with Ultrasonic Temperature Measurement due to Receiver Heating

Mateusz Malinowski

November 4, 2003

1 Introduction

This report seeks to eplain the source of the difficulties encountered when measuring the temperature of a piece of Schott Ceran glass ceramic using piezolectric transducers. It references work documented in a previous report ("Piezoelectric Transducers and Schott Ceran Glass Ceramic") and clarifies some of the results contained therein, concluding that piezoelectric transceivers cannot be effectively used to measure the temperature across a burner in a Schott Ceran glass-ceramic cooktop.

Figure 1: Photograph of experimental setup. The transmitter is on the left, while the receiver is on the right.

The experimental setup used to conduct the temperature measurements consisted of two pieces of PZT (lead zirconate titanate), one acting as a transmitter and the other as a receiver. The two were bonded to a plate of Schott Ceran glass ceramic with two-part epoxy adhesive 30cm apart from each other, which

corresponded to the distance accross a burner. The transmitter was driven directly by a function generator with several cycles of an ultrasonic sine wave, while the receiver output was amplified and passed through a state-variable bandpass filter. The "burner area" between the transmitter and the receiver was heated using either a hot-air gun or an electric stove burner. The experimental setup is illustrated in Figure 1.

2 Measurements

The only effective method of measuring the temperature that emerged from the initial investigation involved correlating the output waveforms at different temperatures with the room-temperature output waveform, in order to quantify an observed phase delay effect. As the glass plate heated, the output waveforms would exhibit decreased amplitudes and an ever greater phase shift with respect to the room-temperature waveform (assumed to be due to the interference of different wave packets). Resultingly, the root-mean-squared magnitude of the cross-correlation of the room-temperature waveform with a given output waveform would decrease with temperature.

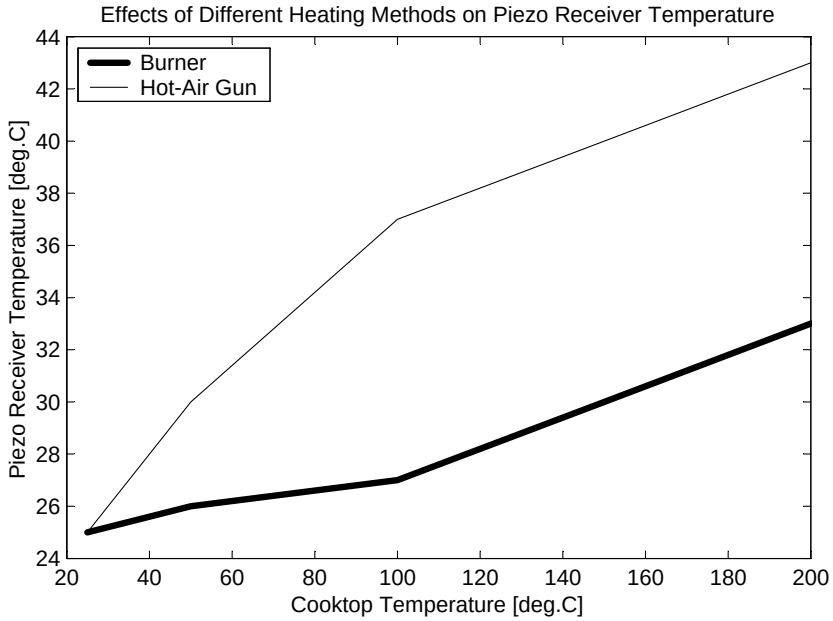

Figure 2: The temperature of the piezoelectric receiver is much higher when heated with the hot-air gun, for the same burner area temperature

It became apparent, however, that similar effects (decrease in amplitude and an increase in phase delay) were present when it was primarily the piezoelectric receiver that was being heated, and not the burner area of the glass. While most of the tests to date had been done with a hot-air gun from above, the final

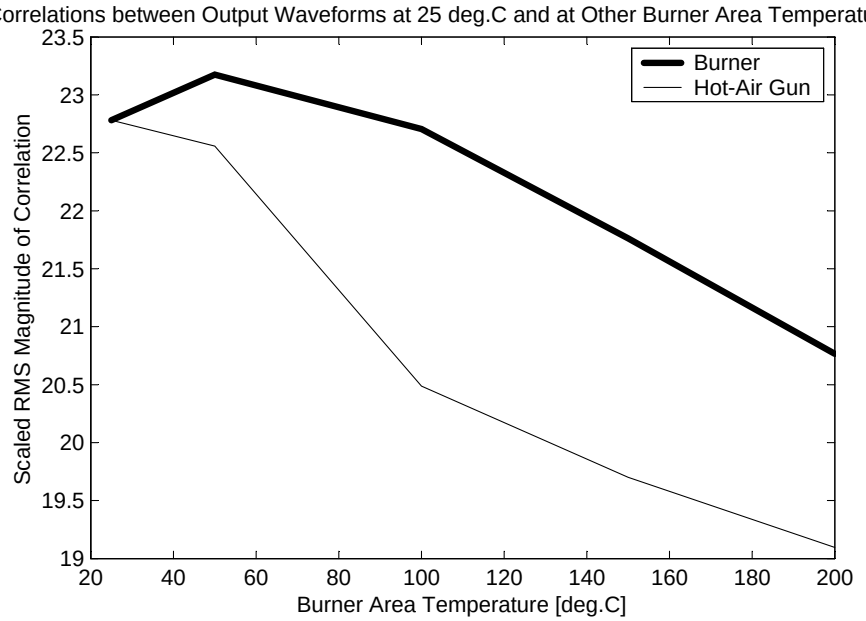

Figure 3: The relationship between the RMS magnitudes of the output waveform correlations at different temperatures of the burner area is ambiguous. What is more, the relationship differs depending on the heating method.

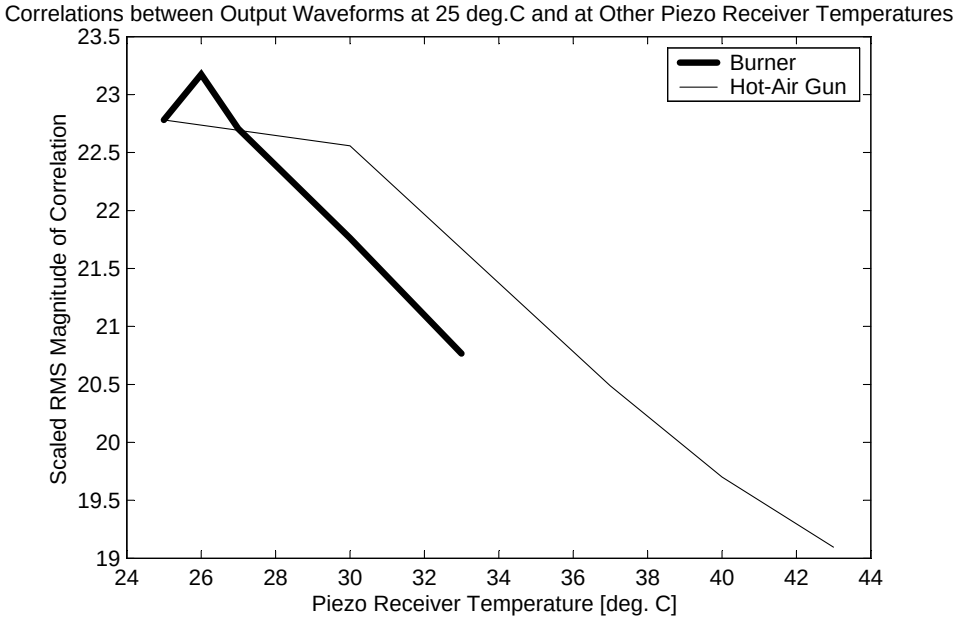

Figure 4: If one ignores the low-temperature irregularities and the constant offset, the relationship between correlation magnitudes and piezo temperature is almost linear and consistent across heating methods.

application would rely on an electric burner from below. The concern was that the phase-delay effect that was to form a basis for any temperature measurement was an artifact of the heating of the receiver by the indiscriminate stream of hot air from the gun.

The suspicion was confirmed by further measurements. An experiment that directly compared the effects of the burner and the hot-air gun revealed that the correlations were indeed related through the temperature of the receiver and not the temperature of the burner area.

As can be seen in Figure 2, the receiver temperature is much higher relative to the burner area when heating with the hot-air gun than when heating with the burner. When one tries to correlate the output waveforms at different temperatures of the burner area, there is no consistency between the burner and hot-air gun heating methods (see Figure 3). When one looks at the correlations versus the piezo receiver temperature, however, the relationship is the same, regardless which heating method is used. Figure 4, illustrates this observation: the slopes of the two graphs are the same, despite some irregularities at lower temperatures.

3 Conclusion

After searching for ways to measure the temperature of Schott Ceran glass ceramic using piezoelectrically stimulated vibrations, the phase delay due to interference effects was discovered to be the most significant effect. The best way to quantify this effect is to cross correlate the waveforms at different temperatures. Unfortunately, as further experiments reveal, the cross correlations, and subsequently the apparent phase delays, depend on the piezo receiver temperature, and not the burner temperature. Measurements of ultrasonic vibrations through the glass ceramic cannot therefore be used to ascertain the temperature of the glass above the burner.